ANNUAL REVIEWS

Annual Review of Fluid Mechanics

Mixing Versus Stirring

Emmanuel Villermaux[1,2]

[1]Aix Marseille Université, CNRS, Centrale Marseille, IRPHE UMR 7342, 13384 Marseille, France; email: emmanuel.villermaux@univ-amu.fr

[2]Institut Universitaire de France, 75231 Paris, France

Annu. Rev. Fluid Mech. 2019.51:245-273. Downloaded from www.annualreviews.org
Access provided by University of Oslo - Medical Library on 06/03/20. For personal use only.

Annu. Rev. Fluid Mech. 2019. 51:245–73

First published as a Review in Advance on September 5, 2018

The *Annual Review of Fluid Mechanics* is online at fluid.annualreviews.org

https://doi.org/10.1146/annurev-fluid-010518-040306

Copyright © 2019 by Annual Reviews.
All rights reserved

ANNUAL REVIEWS CONNECT
www.annualreviews.org
• Download figures
• Navigate cited references
• Keyword search
• Explore related articles
• Share via email or social media

Keywords

mixing, stirring, blending, diffusion, transport, statistical mechanisms

Abstract

Mixing is the operation by which a system evolves under stirring from one state of simplicity—the initial segregation of the constituents—to another state of simplicity—their complete uniformity. Between these extremes, patterns emerge, possibly interact, and die sooner or later. This review summarizes recent developments on the problem of mixing in its lamellar representation. This point of view visualizes a mixture as a set of stretched lamellae, or sheets, possibly interacting with each other. It relies on a near-exact formulation of the Fourier equation on a moving substrate and allows one to bridge the spatial structure and evolution of the concentration field with its statistical content in a direct way. Within this frame, one can precisely describe both the dynamics of the concentration levels in a mixture as a function of the intensity of the stirring motions at the scale of a single lamella and the interaction rule between adjacent lamellae, thus offering a detailed representation of the mixture content, its structure, and their evolution in time.

MÉLANGE: Il se dit de l'aggrégation de plusieurs choses diverses.

—Diderot & d'Alembert, *Encyclopédie* (1765)

1. MIXING IS NEITHER BLENDING NOR STIRRING

Mixing is the science describing the evolution of the concentration content of a deforming continuum substrate in various substances (tracers, chemicals, heat, bacteria, etc.). The subject matter is all contained in **Figure 1*a***, which shows an initially concentrated blob of dye being progressively incorporated into its diluting environment as the medium is stirred down to where none of the constituents of the blob and of the diluting phase can be distinguished; at this point, the dye and diluting environment are mixed.

Mixing is the operation by which a system evolves from one state of simplicity—the initial segregation of the constituents—to another state of simplicity—their complete uniformity. Between these two extremes, patterns emerge (depending on how the medium is deformed), possibly interact (depending on how the mixture disperses in space), and die sooner or later (depending on how Brownian noise has blurred the patterns along the way). As such, mixing is a paradigm of irreversible phenomena (Gibbs 1902).

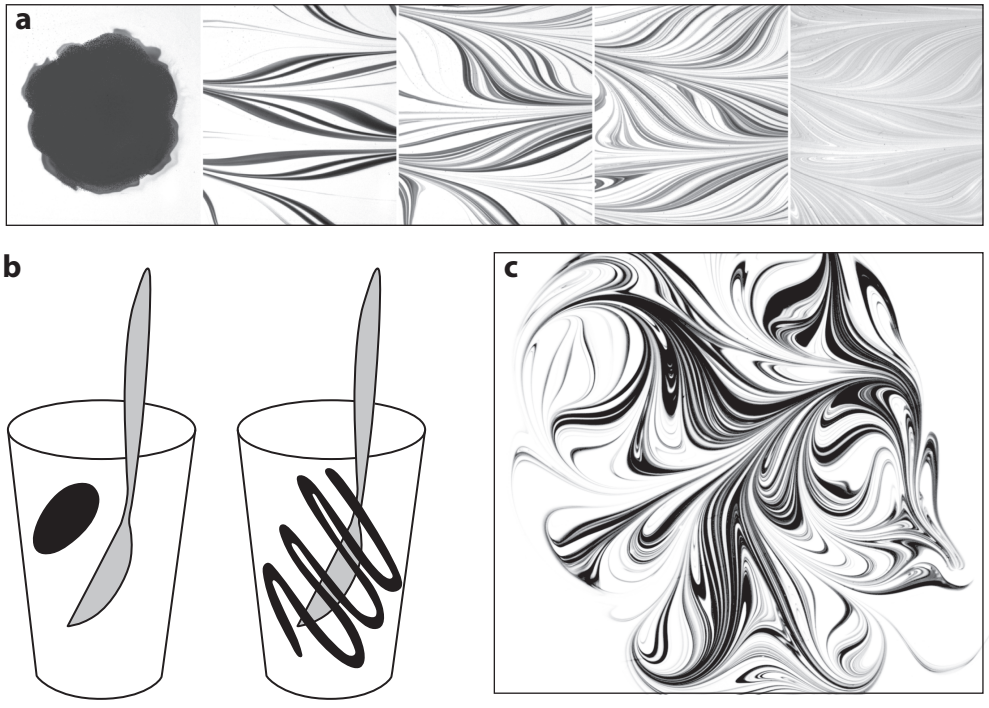

Figure 1

(*a*) A blob of ink deposited in glycerol is stirred by the sequential passage of a rod, like a straw in a milkshake. Stretched lamellae form, get thinner, and overlap as concentration differences fade away across the stirring cycles. Panel *a* adapted with permission from Villermaux & Duplat (2003). (*b*) This celebrated picture, adapted from the very influential book by Arnold & Avez (1967), illustrates blending, not mixing, although the authors used the word "mixing" to refer to iterated maps distorting/spreading a blob in pieces with uniform spatial probability. (*c*) A typical random mixture in two dimensions. A solitary strip unevenly stretched presents broad concentration fluctuations and overlaps with itself in some places of the bounded stirring area.

Annu. Rev. Fluid Mech. 2019.51:245-273. Downloaded from www.annualreviews.org
Access provided by University of Oslo - Medical Library on 06/03/20. For personal use only.

1.1. Concentrations, Intermolecular Scale, and Fluctuations

Mixing deals with concentration fields, not with discrete particles. We first discuss the relationship between the spatial density of particles diffusing on a substrate, and the associated length scales when the substrate is stirred, to ensure the validity of a continuum description.

1.1.1. Concentrations. From a set of discrete particles sparsely spread out in space with interparticle distance λ, a number density $1/\lambda^3$ can be defined from their (molar) concentration c as

$$c = \frac{1}{\mathcal{N}\lambda^3}, \qquad 1.$$

where $\mathcal{N} \simeq 6.02 \times 10^{23}$ is the Avogadro number. For, say, molecules of a chemical species diluted in a liquid with concentration $c = 10^{-1}$ mol/L, we have $\lambda \approx 10^{-8}$ m, a distance 10 to 100 times larger than the typical size of the molecules. A well-defined c thus requires an averaging volume with size η substantially larger than λ. There are, in the mean, $\langle n \rangle \sim (\eta/\lambda)^3$ molecules randomly placed in this volume, with a relative number Poisson fluctuation of order

$$\frac{\sqrt{\langle n^2 \rangle - \langle n \rangle^2}}{\langle n \rangle} \sim \frac{1}{\sqrt{\langle n \rangle}}. \qquad 2.$$

A representative concentration c defining a continuum exempt from trivial particle number fluctuations thus requires that η be substantially larger than λ.

In continuous media, discrete particles suffer Brownian agitation, giving rise to the phenomenon of diffusion, whose intensity is measured by the diffusion coefficient D. For instance, D is given by $(k_B T)^{3/2}/(a^2 p\sqrt{m})$ in a gas of molecules with size a and mass m at pressure p and temperature T, where k_B is the Boltzmann constant, or $k_B T/(6\pi\mu a)$ in a liquid with shear viscosity μ (Landau & Lifshitz 1987). When released around a point in a medium at rest, a set of particles will spread in a time t over an isotropic cloud of radius $\sqrt{Dt}$, and if the medium is deformed (elongated and compressed) at a rate γ, we show in Section 2.4 that spreading is arrested in the compressive direction when the cloud has reached a transverse size

$$\eta = \sqrt{D/\gamma} \qquad 3.$$

called the Batchelor (1959) scale. The condition for a smooth, well-defined concentration field in a mixture is thus that the diffusion length $\sqrt{D/\gamma}$ is larger than the intermolecular distance of the species being mixed (we see in Section 4.3.1 that this occurs at an even larger scale in complex mixtures); in other words, the Péclet number,

$$Pe_\lambda = \frac{\gamma\lambda^2}{D}, \qquad 4.$$

must be smaller than unity. In liquids where the diffusion of big molecules is slow ($D \sim 10^{-9}$ m^2/s or less), the Batchelor scale may be as small as a micron (10^{-6} m) while still remaining large enough to fulfill the condition of a continuum. The concentration, or scalar field, c is then ruled by the conservation equation,

$$\partial_t c + \nabla\cdot(\mathbf{v}\, c) = D\nabla^2 c, \qquad 5.$$

under the action of the stirring velocity field $\mathbf{v}$, which may not be divergence-free (i.e., $\nabla \cdot \mathbf{v} = 0$), and may or may not depend on c itself. The latter case is termed passive scalar mixing. The word "scalar," as opposed to "vector" [although results very similar to those discussed here exist for the magnetic field in two-dimensional (2D) flows; see Moffatt (1983) and Childress & Gilbert (1995)], was employed, presumably for the first time in this context, by L. Kovasznay in 1961 at the Marseille symposium on the "Mechanics of Turbulence" (Favre 1962).

Annu. Rev. Fluid Mech. 2019.51:245-273. Downloaded from www.annualreviews.org
Access provided by University of Oslo - Medical Library on 06/03/20. For personal use only.

1.1.2. The need for distributions of concentration. Examples abound showing that, in most instances involving a mixing operation, it is not the mean concentration of the mixture $\langle c \rangle$ that is of interest, or even the standard deviation $\sqrt{\langle (c - \langle c \rangle)^2 \rangle}$ about the mean (Danckwerts 1952), but rather the probability of an extreme concentration event. For example, the size of a combustion chamber or of a chemical reactor will be set by the residence time of the mixture for the strongest (according to a desired criterion) concentration fluctuation to be erased (Marble 1964). Inhabitants living close to a leaking nuclear or chemical plant care about whether the concentration of pollutants in the effluents released by the leak, in the air or through the ground (Csanady 1973), will be above or below the lethal dose when the pollutant plume reaches them, even if it is once in a lifetime. A residual imperfection in the additives' composition in glass or cement will be the weak link spoiling, e.g., their mechanical resistance (Vidick 1989). Even the lifetime of liquid films as in sea bubbles is presumed to be set by highly concentrated impurities occurring with low probability in the liquid (Poulain et al. 2018).

Conversely, it is sometimes fortunate that a substance or a blend transported by a flow has not yet mixed, as patchy, intermittent concentrated regions might provide vital clues: Bacteria (Berg 2004), moths (Mafra-Neto & Cardé 1994), and lobsters (Koehl et al. 2001) direct their motion toward the source of pheromones or nutrients by sensing their concentration only above a critical detection level (Schnitzer et al. 1990), which may be much higher than the mean concentration in the medium (Celani et al. 2014). The chemical composition of the rocks in the lithosphere, which is homogeneous along stripes but segregated from the rest of the mantle because it is yet unmixed, offers precious clues about the early interior of the Earth (Allègre & Turcotte 1986).

This pressing reality, in conjunction with the fact that in science a satisfactory theory of a physical phenomenon requires a statistical description [Shraiman & Siggia (2000); for instance, think of the kinetic theory of gases (Maxwell 1867) or of Brownian motion (Chandrasekhar 1943, Reif 1965)], leads us to focus on the distribution of concentration of the mixture $p(c)$, also called the probability density function, such that

$$p(c)\,\mathrm{d}c \qquad 6.$$

is the probability of finding in the mixture a concentration level between c and $c + \mathrm{d}c$; obviously, we have $\int p(c)\,\mathrm{d}c = 1$. The goal is to understand the construction mechanisms of $p(c)$ and to relate them to the detailed microscopic processes occurring in the mixture. The distribution $p(\Delta c)$ of the concentration increments $\Delta c(\Delta \mathbf{x}) = \langle c(\mathbf{x} + \Delta \mathbf{x}) - c(\mathbf{x}) \rangle$ is a quantity of general interest that presents original scaling properties (Kraichnan 1994, Falkovich et al. 2001) that we also consider below.

1.2. Semantics, Misconceptions, and the Singular Role of Diffusion

The subject matter is associated with a number of preconceptions and mental images that we consider now.

1.2.1. Semantics. An object may be defined by its opposite, and before we proceed to explain what mixing actually is, let us explain what it is not.

- Mixing is not blending, although a mixture is likely to mix well if it has been homogeneously blended. A perfectly well blended mixture might not be mixed at all if the constituents remain segregated from each other, even within finely divided domains. Mixing requires concentration homogeneity at the molecular scale, λ. Imagine, for example, a mixture of particles with zero diffusivity ($D = 0$, an illusory limit in nature) that has been prepared in such a way that regions marked with $c = 1$ are adjacent to regions marked with $c = 0$.

Annu. Rev. Fluid Mech. 2019.51:245-273. Downloaded from www.annualreviews.org
Access provided by University of Oslo - Medical Library on 06/03/20. For personal use only.

The marked regions are in relative proportion, $\langle c \rangle$. The concentration distribution of the mixture is

$$p(c) = (1 - \langle c \rangle)\,\delta(c - 0) + \langle c \rangle \delta(c - 1) \qquad 7.$$

and remains unchanged whatever the spatial reorganization of the field and the division state of the mixture may be; indeed, whatever $\mathbf{v}$ may be, provided it is incompressible (i.e., $\nabla \cdot \mathbf{v} = 0$, no net expansion or contraction of the substrate), c is ruled by $\partial_t c + \mathbf{v} \cdot \nabla c = 0$ and is conserved along Lagrangian trajectories. There is, in this instance, no mixing at all. There would be for $D \neq 0$, and in that case, sustained motions of the substrate would ultimately lead to

$$p(c) \xrightarrow[t \to \infty]{} \delta(c - \langle c \rangle) \qquad 8.$$

or approach this perfectly well mixed limit after a mixing time, which should be understood in terms of the nature of the stirring motions.

- Mixing is not stirring, although a vigorously stirred mixture will reach homogeneity faster than a mixture kept at rest, which is sensitive to the typically slow (these adjectives will be quantified later) molecular diffusion only. Stirring may contribute to efficient blending, as in **Figure 1*b***, but stirring alone will not mix for the reason underlined above [see the lucid statements by Brodkey (1967) and Epstein (1990)].

1.2.2. The singular role of diffusion. Mixing is stretching-enhanced diffusion: Concentration change ($\partial_t c$) results from a subtle coupling between advection ($\mathbf{v} \cdot \nabla c$) and diffusion ($D\nabla^2 c$) in Equation 5, and fluctuations about the mean will decay according to (Zel'dovich 1937)

$$\frac{\mathrm{d}}{\mathrm{d}t}\left(\langle c^2 \rangle - \langle c \rangle^2\right) = -2D\langle (\nabla c)^2 \rangle \qquad 9.$$

only if D is nonzero. This singular role of molecular diffusion and its coupling with substrate motions are familiar, particularly in the context of dispersion. It is known that without diffusion, the second moment of the residence time distribution of a tracer dispersing along a laminar pipe (with radius b and mean velocity U) diverges. It is finite, with an effective longitudinal dispersion coefficient $D_{\text{eff}} \sim DPe^2$ with $Pe = Ub/D$ as soon as Pe is finite (Taylor 1953). In cellular flows, like along an array of stationary convection cells, the only way a dye can jump from one cell to the other is by crossing their separatrices by molecular diffusion, and in that case, D_{eff} is approximately $D\sqrt{Pe}$ (Shraiman 1987, Solomon & Gollub 1988, Biferale et al. 1995), a conclusion that also holds for reactive mixtures (Audoly et al. 2000). Periodic oscillations of the separatrix location allow cells to exchange material according to a mechanism imagined by Melnikov in 1963 (Rom-Kedar et al. 1990), but this lobe dynamics will by itself not alter the mixture composition (Beigie et al. 1991). In layered systems like porous rocks with broad permeability distributions, it is the diffusion across the layers that regularizes the dispersion process along the layers, which otherwise would be purely ballistic (Matheron & de Marsilly 1980, Bouchaud & Georges 1990). The existence of diffusion, even by a tiny amount, changes the paradigm.

1.2.3. History matters. If mixing is contingent upon diffusion, a frequent underlying assumption, not firmly formalized as such (Sturman et al. 2006, Aref & al. 2017), is that since stirring and diffusion are in essence two different phenomena (which is true), it is therefore paramount to focus on how material particles are advected, because an imitation of a diffusion can always be incorporated in the end of the advection process by some local coarsening to account for the smearing of the (as yet unmixed) scalar field. This sequential vision is fundamentally incorrect, as we show in the sidebar titled History Matters: An Example, illustrated in **Figure 2**. The whole

Annu. Rev. Fluid Mech. 2019.51:245-273. Downloaded from www.annualreviews.org
Access provided by University of Oslo - Medical Library on 06/03/20. For personal use only.

HISTORY MATTERS: AN EXAMPLE

A blob of size s_0 is deposited at $t = 0$ on a 2D substrate. At the same time that the blob diffuses, we stretch the medium so that the blob elongates in one direction and compresses in the other direction down to, say, one tenth of its initial size. We do this according to two distinct protocols, *a* and *b*. In protocol *a*, we first squeeze the blob within a short time according to $s(t) = s_0(1 - t/\epsilon)$, down to $s(t_\epsilon)/s_0 = \epsilon$, and then leave it alone up to $t = 1$ (in units of the blob pure diffusion time, s_0^2/D). In protocol *b*, we leave the blob alone during a time $1 - t_\epsilon$ and then squeeze it in the same way as protocol *a* during $t_\epsilon = \epsilon(1 - \epsilon)$. Since ϵ is much less than 1, the squeezing motion is at large Péclet number, $Pe = \epsilon^{-1}$. The deformation kinematics of the blobs are identical in both protocols, and in the absence of diffusion, both protocols would be indistinguishable. But diffusion has operated along the way, and it is not difficult to see that protocol *a* is more efficient at decaying the concentration in the stretched blob than protocol *b*, in which the blob has remained thick for most of the time. We see in Section 2.3 that the maximal concentration of the blob is given by $\mathrm{erf}(1/4\sqrt{\tau})$, with $\tau \sim \int_0^1 dt'/s(t')^2$, and **Figure 2** demonstrates that in protocol *a*, $\tau \sim \epsilon^{-2}$ is 50 times larger than in *b*, where $\tau \sim 2$. The blob concentration is therefore 2.6 times larger in *b* than in *a* at $t = 1$ for $\epsilon = 0.1$, a ratio that is even larger for a smaller ϵ. History matters.

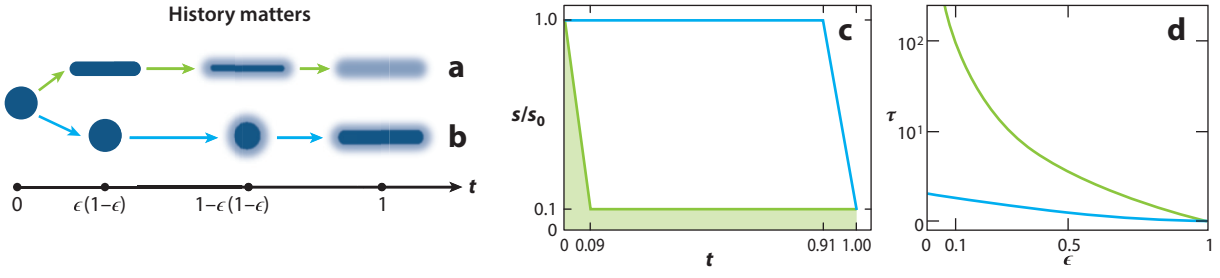

Figure 2

Two kinematically identical deformation protocols of a diffusing blob and their very different mixing states at $t = 1$, as described in the sidebar titled History Matters: An Example.

stretching history, inherently coupled with the permanent but possibly enhanced or slowed-down action of diffusion, has to be accounted for in a precise representation a mixture's fate.

1.3. Approach and Scope

This review summarizes the recent developments in the problem of mixing in its lamellar representation (Batchelor 1959, Ranz 1979, Ottino 1982). This point of view visualizes a mixture as a set of stretched lamellae, or sheets, possibly interacting with each other. It is extremely powerful since it relies on a near-exact formulation of the Fourier equation on a moving substrate (Equation 5) and because it allows one to bridge the spatial structure and evolution of the concentration field with its statistical content in a direct way (Meunier & Villermaux 2003). Within this frame, one can precisely describe both the dynamics of the concentration levels in a mixture as a function of the intensity of the stirring motions at the scale of a single lamella and the nature of the interaction rule between adjacent lamellae (Villermaux & Duplat 2003). This offers a detailed description

Annu. Rev. Fluid Mech. 2019.51:245-273. Downloaded from www.annualreviews.org
Access provided by University of Oslo - Medical Library on 06/03/20. For personal use only.

of the mixture concentration content $p(c)$ (Duplat & Villermaux 2008), its structure $p(\Delta c)$ (Le Borgne et al. 2017), and their evolution in time.

2. STRETCHING-ENHANCED DIFFUSION

Because the displacement gradients of the stirring motion typically form elongated structures (lamellae in 2D and sheets in 3D) from an initially compact isotropic blob passively advected by the flow, concentration gradients are usually only notable in the direction perpendicular to the direction of elongation [with the exception of rare, highly curved regions of the scalar support (Thiffeault 2004), which are ever rarer as stirring proceeds (Meunier & Villermaux 2010)]. This is the reason why a 1D description of the local concentration field dynamics is relevant, as it captures the essence of the coupling between stretching rate and scalar decay.

2.1. Diffusion on Still and Moving Substrates

We first recall when and how stirring the substrate affects diffusion.

2.1.1. Still substrate. The concentration $c(x,t)$ at position x and time t of N diffusing particles released at the origin of an axis at $t=0$, i.e., $c(x,0)=N\delta(x)$, is given by (Fourier 1822)

$$c(x,t)=\frac{N}{2\sqrt{\pi Dt}}e^{-\frac{x^2}{4Dt}}, \tag{10.}$$

while if $N=c_0s_0$ particles have been deposited with uniform concentration c_0 in the interval $x\in\{-s_0/2,s_0/2\}$ at $t=0$, like for a blob of width s_0, one has by integration of the Green's function $c(x-x',t)$ in Equation 10 on the interval (see, e.g., Carslaw & Jaeger 1986)

$$c(x,t)=\frac{c_0}{2}\left[\mathrm{erf}\left(\frac{x+s_0/2}{\sqrt{4Dt}}\right)-\mathrm{erf}\left(\frac{x-s_0/2}{\sqrt{4Dt}}\right)\right]. \tag{11.}$$

The long time limit $\sqrt{Dt}\gg s_0$ of Equation 11 recovers Equation 10. The maximal concentration $c(0,t)\equiv\theta(t)$ at the center of the blob at $x=0$ is

$$\theta(t)=c_0\mathrm{erf}\left(\frac{s_0/2}{\sqrt{4Dt}}\right) \tag{12.}$$

$$\sim\frac{c_0s_0}{\sqrt{Dt}}\quad\text{for}\quad t\gg t_s\simeq\frac{s_0^2}{D}, \tag{13.}$$

an asymptotic trend expressing mass conservation that generalizes to d dimensions as $\theta(t)\sim c_0(s_0/\sqrt{Dt})^d$, which holds after the d-independent mixing time $t_s\simeq s_0^2/D$, beyond which the concentration in the blob departs appreciably from its initial value to reach the asymptotic decay.

The discussion below is not affected by the particular choice we have made for the initial condition in Equation 11, which is only meant to isolate a blob with uniform concentration from its diluting environment where $c=0$. A blob defined by a Gaussian concentration profile of width s_0 (Meunier & Villermaux 2010), or any other shape, leads to identical considerations.

2.1.2. Moving substrate. On a stirred substrate, diffusion competes with the deformation of the medium. The diffusion flux $-D\nabla c$ is proportional to the concentration gradient, which is essentially the concentration difference between two points. If these points get further apart, like in the stretching directions of the substrate, the gradient and the flux decay. In compressive

Annu. Rev. Fluid Mech. 2019.51:245-273. Downloaded from www.annualreviews.org
Access provided by University of Oslo - Medical Library on 06/03/20. For personal use only.

regions, the gradient steepens, and the diffusion flux is enhanced. For this key mechanism to operate, substrate compression must be fast enough.

Any kind of shear motion will elongate a blob into a lamella whose width is, say, of order s. The lamella will decay by transverse diffusion according to Equation 10 in a time s^2/D. If, at the same time, the substrate is compressed at a rate γ such that $\dot{s}$ equals $-\gamma s$, it is clear that γ^{-1} should be smaller than s^2/D for gradient reinforcement to be effective. Thus, starting with a blob of size s_0, mixing will amount to a simple diffusion problem if s_0^2/D is much less than γ^{-1}, and a genuine nontrivial coupling will occur when s_0^2/D is much greater than γ^{-1}, that is, when the Péclet number

$$Pe = \frac{\gamma s_0^2}{D} \qquad 14.$$

is larger than unity.

2.2. The Ranz Transformation

In a local Lagrangian frame (x, y) moving with a lamella [in 2D; the discussion is readily generalized to a sheet in 3D (Martinez-Ruiz et al. 2018)] such that the direction x points in the direction of the maximal concentration gradient and y is perpendicular to it [these directions tend to align with the eigenvectors of the deformation tensor; see Ashurst et al. (1987)], the components (u, v) of the velocity field $\mathbf{v}$ in Equation 5 are related to the compression rate of the (incompressible, $\nabla \cdot \mathbf{v} = 0$) substrate material particles by $u = (\dot{s}/s)x$ and $v = -(\dot{s}/s)y$.

Given the discussion above on the relative magnitude of the concentration gradients in the elongating and compressing directions of the substrate, we see that the local dynamics of the concentration field from Equation 5,

$$\partial_t c + u\partial_x c + v\partial_y c = D\left(\partial_x^2 + \partial_y^2\right) c, \qquad 15.$$

incorporates two subdominant terms. When stretched at large Pe, a blob of initial surface s_0^2 is elongated into a strip of width s and length $\ell \gg s$ (see **Figure 3**) so that, by incompressibility, s_0^2 is approximately $s \times \ell$. The orders of magnitude of the components of the concentration gradient are $\mathcal{O}(\partial_x c) = 1/s$ and $\mathcal{O}(\partial_y c) = 1/\ell$. Thus, in a neighborhood of size s at the center of the strip, $\mathcal{O}(|u\partial_x c|/|v\partial_y c|) = \ell/s$ is much greater than 1, and for the same reason, $\mathcal{O}(|\partial_x^2 c|/|\partial_y^2 c|) = (\ell/s)^2$ is also much greater than 1. The near-exact form (at large Pe) of the evolution equation for c is thus

$$\partial_t c + (\dot{s}/s)\, x\, \partial_x c = D\partial_x^2 c. \qquad 16.$$

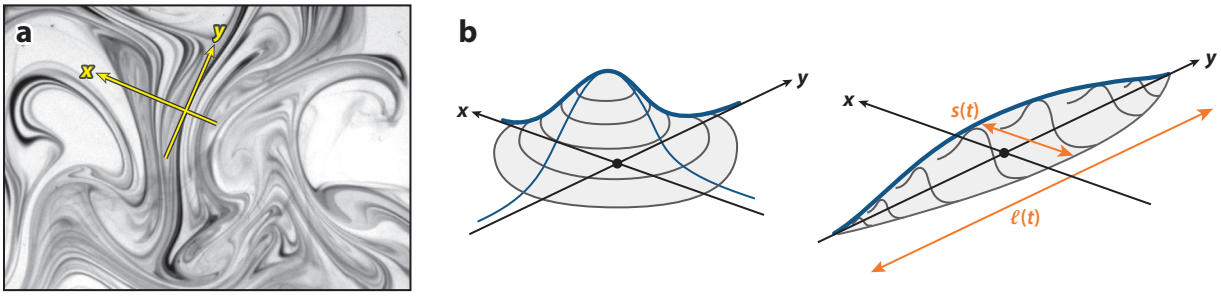

Figure 3

Diffusion on a moving substrate. A blob that would otherwise expand isotropically is stretched along y and compressed along x, the permanent process forming lamellae in stirred mixtures.

Annu. Rev. Fluid Mech. 2019.51:245-273. Downloaded from www.annualreviews.org
Access provided by University of Oslo - Medical Library on 06/03/20. For personal use only.

As it is, Equation 16 already represents considerable progress since it bridges, by a linear equation, the dynamics of c with the prescribed kinematics of the stirring field through a single feature, namely the compression rate $\dot{s}/s$. This compression rate reflects, in incompressible flows, the growth rate of material lines length (i.e., $\dot{\ell}/\ell$) or the area of surfaces.

More can be done to improve understanding of Equation 16 and make it more practical to use. Distance x and time t define the space in which we discuss physical phenomena, but they are not necessarily the natural coordinates. A coordinate change, popularized by Marble & Broadwell (1977) and Ranz (1979), in which distances are measured in units of s and time in units of the diffusion time s^2/D such that

$$\xi = \frac{x}{s(t)} \quad \text{and} \quad \tau = D\int_0^t \frac{\mathrm{d}t'}{s(t')^2}, \tag{17.}$$

transforms Equation 16 into a pure diffusion equation:

$$\partial_\tau c = \partial_\xi^2 c. \tag{18.}$$

This extremely elegant and useful result is consistent with the fact that only molecular diffusion can alter the concentration content of a field. Ultimately, the dynamics of c complies with pure diffusion; the dilatation or compression of space [i.e., the time dependence of $s(t)$] is just a way to delay or hasten the process. Since $s(t)$ typically decreases in time by stirring, τ in Equation 17 increases faster than linearly in time, expressing the expected acceleration of diffusion.

Either in its original form or in slightly different forms, Equation 18 has been put to use in various disciplines, including heat transfer (Levèque 1928), turbulence (Batchelor 1959), reacting flows (Gibson & Libby 1972, Carrier et al. 1975, Marble 1988), engineering and process industry (Mohr et al. 1957, Ranz 1979), geophysics (Rhines & Young 1983, Allègre & Turcotte 1986), chaos (Ottino 1982, Beigie et al. 1991), physics (Moffatt 1983), and mathematics (Fannjiang et al. 2004).

From a blob or strip of initial transverse size s_0, the concentration (scaled by c_0) in the genuine coordinates (Equation 17) is given by

$$c(\xi,\tau) = \frac{1}{2}\left[\mathrm{erf}\left(\frac{\xi+1/2}{2\sqrt{\tau}}\right) - \mathrm{erf}\left(\frac{\xi-1/2}{2\sqrt{\tau}}\right)\right], \tag{19.}$$

which is obtained in the same way as the concentration profile in Equation 11.

2.3. Maximal Concentration and Mixing Time

The maximal concentration in the lamella is found at $x = 0$ (that is, $\xi = 0$) and is

$$\theta(\tau) = \mathrm{erf}\left(\frac{1}{4\sqrt{\tau}}\right) \xrightarrow[\tau\gg 1]{} \frac{1}{\sqrt{\tau}}, \tag{20.}$$

while $\theta(\tau)$ is approximately 1 as long as τ is significantly less than 1. In line with Section 2.1.1, we define the mixing time t_s, beyond which the concentration in the lamella has departed appreciably from its initial value to reach the asymptotic decay $1/\sqrt{\tau}$, by the condition

$$\tau(t_s) = \mathcal{O}(1). \tag{21.}$$

For any stirring protocol involving any particular form of $s(t)$ and therefore of $\tau(t)$, there corresponds a given t_s with, notably, a given dependence on Pe (see the sidebar titled Stirring Protocols and Mixing Times). The mixing time is always of the form

$$t_s \sim \frac{1}{\gamma}\mathcal{F}(Pe), \tag{22.}$$

Annu. Rev. Fluid Mech. 2019.51:245-273. Downloaded from www.annualreviews.org
Access provided by University of Oslo - Medical Library on 06/03/20. For personal use only.

STIRRING PROTOCOLS AND MIXING TIMES

We list below some standard stirring protocols, along with their mixing times t_s from Equation 21 and maximal concentrations $\theta(t)$ from Equation 20 for $t > t_s$, in the large-Pe limit.

- For a simple shear (Ranz 1979), we have $s(t) = s_0/\sqrt{1+(\gamma t)^2}$, providing

$$\tau = \frac{\gamma t}{Pe}\left[1+\frac{1}{3}(\gamma t)^2\right], \quad \text{giving} \quad t_s \sim \frac{1}{\gamma}Pe^{1/3} \quad \text{and} \quad \theta(t) \sim (\gamma t)^{-3/2}.$$

- Elongations in two directions (Okubo & Karweit 1969) with $s(t) = s_0/[1+(\gamma t)^2]$ provide

$$\tau = \frac{\gamma t}{Pe}\left[1+\frac{2}{3}(\gamma t)^2+\frac{1}{5}(\gamma t)^4\right], \quad \text{giving} \quad t_s \sim \frac{1}{\gamma}Pe^{1/5} \quad \text{and} \quad \theta(t) \sim (\gamma t)^{-5/2}.$$

- A stagnation (saddle) point with steady stretching (Batchelor 1959) is such that $s(t) = s_0 e^{-\gamma t}$; thus,

$$\tau = \frac{1}{2Pe}\left(e^{2\gamma t}-1\right), \quad \text{giving} \quad t_s = \frac{1}{2\gamma}\ln(1+2Pe) \xrightarrow[Pe\gg 1]{} \frac{1}{2\gamma}\ln Pe \quad \text{and} \quad \theta(t) \sim e^{-\gamma t},$$

  where it should be noted that the pure diffusive limit $t_s \sim s_0^2/D$ is recovered for $Pe \ll 1$ and that, under stretch, diffusion is arrested in the elongating direction where $\ell(t) = s_0 e^{\gamma t}$, since in that case, we have $\tau = \frac{1}{2Pe}(1-e^{-2\gamma t}) \to 1/2Pe$.
- Sub- ($\alpha < 1$) or super- ($\alpha > 1$) exponential stretching (de Rivas & Villermaux 2016) with $s(t) = s_0 e^{-(\gamma t)^\alpha}$ corresponds to

$$\tau \sim \frac{1}{Pe}\frac{e^{2(\gamma t)^\alpha}}{2\alpha(\gamma t)^\alpha}, \quad \text{giving} \quad t_s \sim \frac{1}{\gamma}(\ln Pe)^{1/\alpha} \quad \text{and} \quad \theta(t) \sim e^{-(\gamma t)^\alpha}.$$

- A finite-time singularity (Villermaux 2012b) such that $s(t) = s_0(1-\gamma t)^\alpha$ with $\alpha > 1/2$ gives

$$\tau = \frac{1-(1-\gamma t)^{1-2\alpha}}{(1-2\alpha)Pe}, \quad \text{giving} \quad \gamma t_s \sim 1 - Pe^{1/(1-2\alpha)} \xrightarrow[Pe\to\infty]{} \alpha > 1/2.$$

  This is the only instance where the mixing time t_s remains strictly finite at $Pe = \infty$ and is given by the singularity time γ^{-1}, at which $s(\gamma^{-1}) = \theta(\gamma^{-1}) = 0$.

where γ relates to the deformation rate of the substrate, and $\mathcal{F}(Pe)$ is a weak function of the Péclet number Pe, typically a small power or a logarithm, a fact that has been known to engineers for a long time (Nagata 1975). Irrespective of the nature of the substance being mixed (i.e., of D), the time it takes to mix a substance in a stirred vessel with a standard impeller rotating $\dot{N}$ rounds per unit of time is $\dot{N}t_s \approx 5$, where the factor 5 reflects geometrical factors and a logarithmic Péclet correction at large Reynolds number, which is so weak that it is insensitive in the engineering practice.

Put differently in terms of an image frequently associated with mixing, it is well known that when stirring a drop of milk in a cup of coffee, only the number of spoon turns matters. This fact is indeed familiar in the turbulence context [at large Reynolds number, the analog of the Péclet number for vorticity (Moffatt 1983)], where the cascade time from the blob injection (of scalar or vorticity) to its dissipation by molecular diffusion or viscosity is essentially independent of them, or involves a weak correction only.

Despite being weak in practice, since a logarithm is close to a constant at large Pe (see, e.g., Donzis et al. 2005), the correction $\mathcal{F}(Pe)$ is nevertheless singular [it is infinite in the limit $D \to 0$,

Annu. Rev. Fluid Mech. 2019.51:245-273. Downloaded from www.annualreviews.org
Access provided by University of Oslo - Medical Library on 06/03/20. For personal use only.

sometimes termed a dissipative anomaly (Falkovich et al. 2001)], and this makes sense: The decay rate of the scalar fluctuations is solely prescribed by the stirring strength γ, but only after the mixing time. In other words, it takes some time for the stretching motions to bring the scalar blob down to a scale small enough for molecular diffusion to become effective in erasing the scalar differences. This time depends on the stirring strength γ, on the initial blob size s_0, and on its diffusional properties D; this is the essence of mixing in stirred media.

After the mixing time, the maximal concentration $\theta(t)$ in Equation 20 decreases according to mass conservation $\theta(t)\sqrt{Dt}/s(t) \sim 1$ as $\theta(t) \sim (\gamma t)^{-\alpha-1/2}$ for power law stretching or $\theta(t) \sim e^{-\gamma t}$ for exponential stretching (see the sidebar titled Stirring Protocols and Mixing Times) and in any case faster than for pure diffusion, where $\theta(t) \sim (Dt)^{-d/2}$ in d dimensions.

2.3.1. The case of small Péclet numbers. We have stressed in Section 2.1.2 that mixing is a nontrivial problem only in the limit of large Péclet numbers, but this is not exactly true. An interesting coupling occurs for $Pe < 1$ in a shear flow: At low Pe, diffusion broadens a (small) blob in its traverse direction as $\sqrt{Dt} > s_0$, which results, since the blob sits in a shear, in a longitudinal dispersion velocity of the blob, $\dot{\ell} \sim \gamma\sqrt{Dt}$, that is, in a blob length scaling of $\ell(t) \sim \gamma\sqrt{D}\,t^{3/2}$ [this is besides a well-known recipe for producing a superdiffusive dispersion law *à la* Richardson (1926); see for instance Celani et al. (2005)]. The blob surface increases as $\sqrt{Dt} \times \ell(t) = \gamma Dt^2$, which, by mass conservation, provides the maximal concentration carried by the blob $\theta(t)$ as

$$\theta(t) \sim \frac{s_0^2}{\gamma Dt^2}. \qquad 23.$$

However, this regime is likely to operate if $\ell(t)$ is larger than the pure kinematic elongation of the blob, $s_0\gamma t$, that is, for $t > s_0^2/D$, a large time compared to $t_s \sim Pe^{1/3}/\gamma$ unless Pe is less than 1. The corresponding regime will thus affect the early dynamics of a blob for, at best, Pe of order unity. A rigorous treatment of this nice exercise is given by Thiffeault (2008).

2.4. Batchelor Scales and Dissipation

We have emphasized how diffusion broadening competes with substrate compression. This process is associated with a length scale η, which we have already alluded to in Section 1.1.1. In fact, there is a family of length scales, all representative of the same phenomenon. For $\tau > 1$, that is, for $t > t_s$, the concentration profile across a lamella (Equation 19) converges toward a decaying Gaussian (de Rivas & Villermaux 2016):

$$c(x,t) \sim \frac{1}{2\sqrt{\pi\tau}} e^{-\frac{x^2}{2\eta^2}}, \qquad 24.$$

$$\text{with} \quad \eta(t) = s(t)\sqrt{\tau(t)}. \qquad 25.$$

We call $\eta(t)$, and more precisely, $\eta(t_s)$, a Batchelor scale. After the mixing time, $\eta(t)$ has no reason to be a constant, in general. It is in the special stirring protocol of a constant stretching rate γ. In that case, we have $s(t) = s_0 e^{-\gamma t}$ and $\tau(t) \sim e^{2\gamma t}/Pe$; therefore, $s(t)\sqrt{\tau(t)} \sim \sqrt{D/\gamma}$ is indeed a constant of time that is also independent of s_0 (Batchelor 1959).

This length scale first arose in turbulence, where the relevant stretching rate, $\gamma = (U/L)Re^{1/2}$, is the one prevailing for scales below the Kolmogorov scale $LRe^{-3/4}$, where $Re = UL/\nu$ is the Reynolds number with a velocity U at the large scale L and a fluid kinematic viscosity of ν. The (original) Batchelor scale, $LRe^{-3/4}Sc^{-1/2}$, where $Sc = \nu/D$ is the Schmidt number, is usually difficult to detect in flows at large Reynolds number and Schmidt number (note that $Pe = Re \times Sc$) because it is small (Miller & Dimotakis 1996); however, it is more easily accessible to precise

Annu. Rev. Fluid Mech. 2019.51:245-273. Downloaded from www.annualreviews.org
Access provided by University of Oslo - Medical Library on 06/03/20. For personal use only.

RULE OF THUMB

The qualitative meaning of the crossover condition in Equation 21 is that diffusion starts to operate when its associated timescale compares to the substrate deformation time, that is, when

$$|\dot{s}/s| \sim D/s^2.$$

Generically taking $s(t)$ to be given by $s_0(\gamma t)^{-\alpha}$, one sees that

$$t_s \sim \frac{1}{\gamma} Pe^{1/(2\alpha+1)} \quad \text{and} \quad \theta(t) \sim (\gamma t)^{-\alpha-1/2},$$

explaining why the Pe dependence of t_s is weaker when the stretching is stronger (i.e., large α).

Annu. Rev. Fluid Mech. 2019.51:245-273. Downloaded from www.annualreviews.org
Access provided by University of Oslo - Medical Library on 06/03/20. For personal use only.

numerical simulations (Schumacher et al. 2005) or to experiments involving moderate and simple deformation fields (Meunier et al. 2015). Anticipating Section 3.2, we note that since in random flows stretching rates are distributed in intensity, the Batchelor scale above has to be understood as a representative mean of an otherwise broad distribution of scalar dissipation scales (Schumacher et al. 2005).

In more general stirring protocols, the compression rate $\gamma(t) = -\dot{s}/s$ is itself time dependent. For instance, if $s(t)$ decreases as a power law like $s(t) \sim s_0(\gamma t)^{-\alpha}$, one has

$$\eta(t) \sim \sqrt{Dt}, \tag{26.}$$

which is consistent with the large time decay of the compression rate, $\gamma(t) \sim 1/t$, which is finally overcome by diffusion broadening. Since, in that case (see the sidebar titled Rule of Thumb) we have $\gamma t_s \sim Pe^{1/(2\alpha+1)}$, then

$$\eta(t_s) \sim s_0 Pe^{-\alpha/(2\alpha+1)}, \tag{27.}$$

which now depends on the value of α and on the initial condition s_0. The case $\alpha = 1$ (shear flow) was precisely investigated by Souzy et al. (2018), who indeed confirmed all the necessary trends and scaling laws (**Figure 4**).

In time-dependent flows, if α is a number reflecting the accelerated nature of the stretch intensity ($\alpha > 1$) or its slowing down ($\alpha < 1$), we have

$$\frac{\gamma(t)}{\gamma} = \alpha\,(\gamma t)^{\alpha-1}, \tag{28.}$$

a formulation that has no fundamental justification other than being easily adaptable to different flow configurations, given that in nature, diverse behaviors exist concomitantly or sequentially (McKenzie 1979). The corresponding Batchelor scale in Equation 27 tends toward

$$\eta(t) \sim \sqrt{\frac{D}{\alpha\gamma}}\,(\gamma t)^{\frac{1-\alpha}{2}} \tag{29.}$$

when $t > t_s$ and coincides with the usual constant value $\sqrt{D/\gamma}$ in exponentially diverging flows with $\alpha = 1$. The concentration gradient continues steepening as the maximal concentration decays in the accelerated regions of the flow [see an example with $\alpha = 2$ by Néel & Villermaux (2018)] and relaxes for slowed-down stretching (de Rivas & Villermaux 2016).

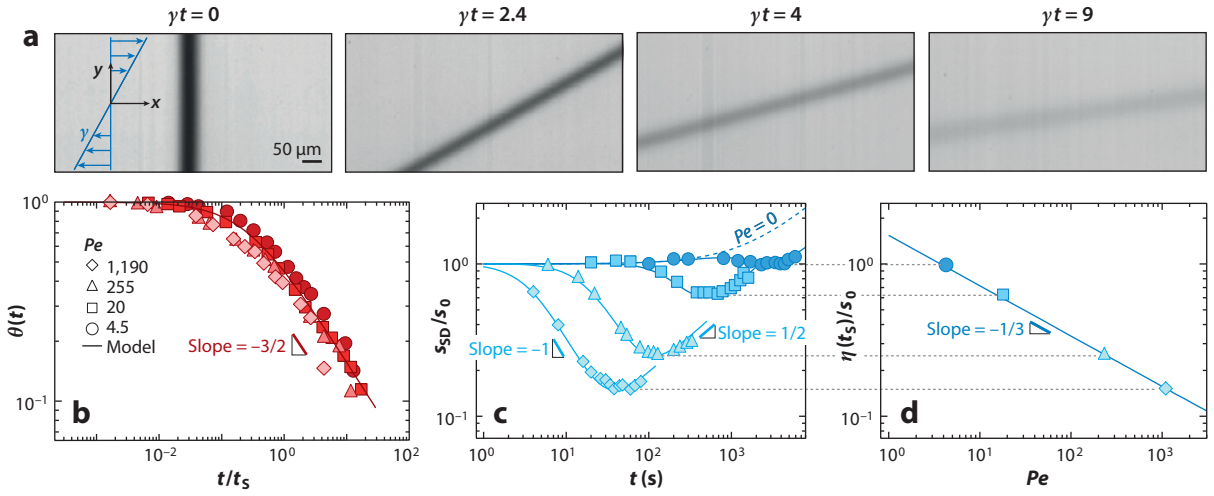

Figure 4

(*a*) Lamella mixing in a shear flow. (*b*) Decay of the maximal concentration, $\theta(t) \sim (t/t_s)^{-3/2}$. (*c*) Standard deviation of the lamella concentration profile s_{SD}/s_0, first showing kinematic compression, followed by diffusive broadening, according to Equation 26. (*d*) Dependence of the Batchelor scale $\eta(t_s)/s_0$ on Péclet number *Pe* in Equation 27 with $\alpha = 1$. Figure adapted with permission from Souzy et al. (2018).

Annu. Rev. Fluid Mech. 2019.51:245-273. Downloaded from www.annualreviews.org
Access provided by University of Oslo - Medical Library on 06/03/20. For personal use only.

2.4.1. Dissipation. There are many global, lumped indices that have been defined to quantify a mixing state or the "mixidness" of a given protocol (its ability to mix well), such as Danckwerts' (1952) intensity of segregation (variance of c about the mean), Kitanidis' (1994) dilution index [entropy of $p(c)$], and Mathew et al.'s (2005) mix-norm [field coarsening; see also Thiffeault (2012)]. These are all ersatz of the concentration distributions $p(c)$ (see Le Borgne et al. 2015). Among these indices is the dissipation rate, $\chi(t) = -2D\langle(\nabla c)^2\rangle$, which is the average squared concentration gradient that, when weighted by D, is the decay rate of the mean squared concentration differences about the mean (see Equation 9 and Zel'dovich 1937).

From the Batchelor scale, $\eta(t)$, and the maximal concentration in a lamella, $\theta(t)$, a typical concentration gradient is $\theta(t)/\eta(t)$, and for an isolated stretching blob at $t \gg t_s$, we have

$$\chi(t) \sim \gamma\sqrt{Pe}\,(\gamma t)^{-\alpha-3/2} \quad \text{(power law stretching)} \qquad 30.$$

$$\text{and} \quad \chi(t) \sim \gamma\sqrt{Pe}\,e^{-\gamma t} \quad \text{(exponential stretching)}, \qquad 31.$$

which not surprisingly exhibit a stronger time dependence than pure diffusion, where $\chi(t) \sim D^{-d/2}t^{-1-d/2}$ in d dimensions.

There is no dissipation as D tends to 0 because t_s tends to infinity in that singular limit (see Section 2.3 and Balmforth & Young 2003). The above relations are readily generalized to nondecaying mixtures where blobs are periodically injected and stirred at steady state (Villermaux 2012b). This is a way to understand eddy diffusivities from elementary principles or heat and mass transfer laws at sheared boundaries.

3. SOLITARY STRIPS

By "solitary strips," we mean lamellae carrying concentration levels (Equation 20) solely prescribed by their local stretching history according to Equation 17. In that case, the concentration

distribution $p(c)$ simply reflects the relative cumulated elongation intensities along the strip at a given time. We examine several examples with either steady or time-dependent stirring protocols.

3.1. Deterministic Stirring

We call stirring protocols deterministic if they are either steady or time dependent but lead to a unique trajectory of the deformed blob for a given initial condition.

3.1.1. The concentration distribution of a Gaussian spatial profile. We aim at giving a representation of the distribution $p(c)$ of the concentration levels c along a lamella distorted by a flow. After the mixing time, these levels are carried by the local Gaussian spatial profile across the lamella in Equation 27 parameterized by its maximum θ and width η; the concentration levels span from 0 far from the lamella to θ. Exploring the c levels over an x-range of the order of a few η along the x-axis across the lamella (see Equation 27), each c level is encountered with a relative frequency given by

$$g(c|\theta) \sim \frac{\eta^{-1}}{|\mathrm{d}c/\mathrm{d}x|_{x(c)}} \sim \frac{1}{c\sqrt{\ln(\theta/c)}}, \qquad 32.$$

with $x(c) \sim \eta\sqrt{\ln(\theta/c)}$. The characteristic U-shape of this distribution is well known (Meunier & Villermaux 2003, 2007, 2010; Duplat et al. 2010a; Martinez-Ruiz et al. 2018; Souzy et al. 2018). However, the distribution Equation 32 is not normalized because of its divergence at $c = 0$, reflecting the free choice in defining the support of the lamella, which can extend arbitrarily far from it in its diluting ocean, a divergence that is thus not physically meaningful. The distribution $g(c|\theta)$ has another divergence at $c = \theta$ that singles out the concentration maximum, and it is this divergence that carries the relevant information in nontrivial flows where θ is itself distributed.

Unless explicitly taken into account when they give rise to an interesting phenomenon (Meunier & Villermaux 2007), the contributions of the low concentration levels from the spatial tail of the Gaussian profile (Equation 27) can usually be disregarded, and thus it is usually fair to approximate Equation 32 as

$$g(c|\theta) \approx \delta(c - \theta), \qquad 33.$$

which serves our purpose of discussing the large excursion shape of the distribution $p(c)$ of a strip along which the maxima θ are distributed.

3.1.2. Mixing by a vortex. The stirring protocol of a permanent point vortex with circulation Γ (azimutal velocity $\Gamma/2\pi r$) is an illustration of the construction mechanism of $p(c)$ worth considering in some detail (Meunier & Villermaux 2003).

A blob of size s_0 is deposited at a distance $\tilde{r} \gg s_0$ from the center of the vortex. An element of surface $s_0\,\mathrm{d}r$ of the blob is stretched kinematically into a strip of length $\mathrm{d}\ell$ such that

$$\mathrm{d}\ell = \mathrm{d}r\sqrt{1 + \frac{\Gamma^2 t^2}{\pi^2 r^4}} \to \mathrm{d}r\frac{\Gamma t}{\pi r^2}, \qquad 34.$$

spiraling around the vortex center. Area conservation, $s_0\mathrm{d}r = s(r,t)\,\mathrm{d}\ell$, thus gives rise to a time- and radius-dependent stretching rate, so that τ in Equation 17 depends on both r and t as

$$\tau(r,t) = \frac{Dt}{s_0^2}\left(1 + \frac{\Gamma^2 t^2}{3\pi^2 r^4}\right), \qquad 35.$$

with a time dependence (i.e., t^3) reminiscent of flows where material line lengths increase in proportion with time (the length of the spiral is $L = \int \mathrm{d}\ell \approx \Gamma s_0 t/\tilde{r}^2$). The condition $\tau(r,t) = \mathcal{O}(1)$

Annu. Rev. Fluid Mech. 2019.51:245-273. Downloaded from www.annualreviews.org
Access provided by University of Oslo - Medical Library on 06/03/20. For personal use only.

Annu. Rev. Fluid Mech. 2019.51:245-273. Downloaded from www.annualreviews.org
Access provided by University of Oslo - Medical Library on 06/03/20. For personal use only.

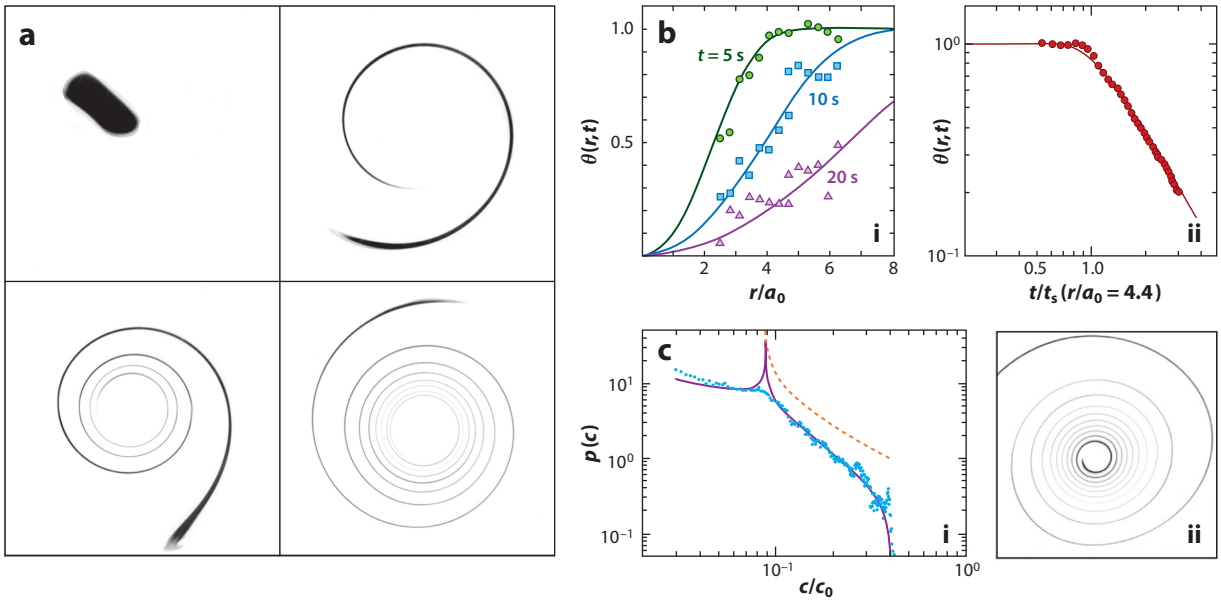

Figure 5

Mixing by a vortex. (*a*) A blob in the far field of a Lamb–Oseen vortex spirals around the vortex. (*b*) The concentration $\theta(r,t)$ of the blob in panel *a* as a function of the radial location r/a_0 at fixed instants in time (*i*) and as a function of time at a fixed radial location (*ii*). The solid lines give the expected values from $\theta(r,t) = \mathrm{erf}[1/\sqrt{4\tau(r,t)}]$, where $\tau(r,t)$ is given by Equation 35. (*c*) Subpanel *i* shows the concentration distribution $p(c)$ and the expected law (*solid line*) of a spiraling blob at a fixed time, exhibiting a Van Hove singularity when the blob is deposited close to the viscous core of the vortex shown in subpanel *ii*. Panels adapted with permission from (*a*,*b*) Meunier & Villermaux (2003) and (*c*) Meunier & Villermaux (2007).

provides an r-dependent mixing time:

$$t_s(r) \sim \frac{r^2}{\Gamma}\left(\frac{s_0}{r}\right)^{2/3}\left(\frac{\Gamma}{D}\right)^{1/3}. \qquad 36.$$

The fluid particles of the blob closer to the center of the vortex are stretched faster and hence have a shorter mixing time; they also carry a smaller maximal concentration, $\theta(r,t) = \mathrm{erf}(1/4\sqrt{\tau}) \sim 1/\sqrt{\tau(r,t)}$, because they have mixed earlier (**Figure 5**). The one-to-one correspondence between strip elongation and maximal concentration along the deformed blob translates to the conservation law $q(\theta)\,\mathrm{d}\theta = \mathrm{d}\ell/L$, providing the distribution of maximal concentrations:

$$q(\theta) \sim \frac{\Gamma t}{Lr^2}\frac{1}{|\mathrm{d}\theta/\mathrm{d}r|}. \qquad 37.$$

The full concentration field c can be reconstructed precisely (Meunier & Villermaux 2003) from the elementary U-distributions in Equation 32, which also describe some features like Van Hove singularities when the spatial concentration field presents a saddle point in a variant of the present problem (Meunier & Villermaux 2007). At large times, the use of the approximation Equation 33 is such that $p(c) = \int g(c|\theta)q(\theta)\,\mathrm{d}\theta \approx q(\theta = c)$, and when $t > t_s(r)$ for all $r \in \{\tilde{r}, \tilde{r} + s_0\}$, we have

$$p(c) \sim \left(\frac{s_0}{\sqrt{D}\Gamma t^{3/2}}\right)^{1/2}\frac{\tilde{r}}{c^{3/2}}. \qquad 38.$$

Because the particles close to the vortex center are more stretched, they occupy a larger fraction of the spiral than the remote ones. Since their concentration is smaller, as they are more elongated,

the overall $p(c)$ is a decreasing function of c. This simple fact is the paradigm of solitary strip mixing.

3.2. Random Flows

A construction identical to the one above that relates the strips' elongations to $p(c)$ holds when stirring is time dependent in the sense of being chaotic or turbulent. Irrespective of the stirring protocol, the elongation $\rho(t) = s_0/s(t)$ is related to τ by

$$\tau \approx \frac{Dt}{s_0^2}\rho^2 \quad \text{for} \quad \rho \gg 1, \tag{39.}$$

and since $\theta \sim 1/\sqrt{\tau}$, the knowledge of the distribution of ρ in an ensemble of stretched lamellae provides the distribution of τ (and therefore of t_s) and of θ (and therefore of c) via a simple change of variables.

3.2.1. Sequential elongations: the log-normal paradigm. We consider protocols comprising a sequential, uncorrelated (in intensity and direction) series of stretchings applied either to a large collection of blobs or to subparts of a stretching blob. This can be realized in several ways, like in asymmetrical Baker transforms (Ott & Antonsen 1989) or other iterated maps (Meunier & Villermaux 2010, Figueroa et al. 2014) and random processes (Kalda 2000), by transporting the blob through successive pores in a porous medium (Le Borgne et al. 2015) or in a sheared suspension of beads (Souzy et al. 2017), for instance.

If the blob experiences N successive random stretchings ρ_i, its elongation is $\rho = \prod_i^N \rho_i$, and if the ρ_i's are all independent, the probability $Q(\rho)$ that a point on the initial blob is stretched by a factor ρ is given by $Q(\rho) = \exp[-(\log\rho - N\mu)^2/2N\sigma^2]/\rho\sqrt{2\pi N\sigma^2}$, where μ and σ^2 are the mean and variance of $\log\rho$, respectively, defining a log-normal distribution. The probability $P(\rho)$ that a point on the final strip has experienced a stretching ρ is equal to $[s_0/\ell(t)]\rho\, Q(\rho)$, where $\ell(t)$ is the total length of the strip. With a number N of stretchings proportional to time t in a permanently stirred flow, we have

$$P(\rho) = \frac{s_0/\ell(t)}{\sqrt{4\pi\kappa t}}\, \exp\left[-\frac{(\log\rho - \gamma_p t)^2}{4\kappa t}\right], \tag{40.}$$

where $\gamma_p = N\mu/t$ is the most probable stretching rate and $\kappa = N\sigma^2/(2t)$ stands for their dispersion, both of which depend on the type of unsteadiness in the flow [for instance, Souzy et al. (2017) showed how γ_p and κ depend on the volume fraction of beads in a sheared suspension]. The net length of the strip, $\ell(t) = \int \rho\, Q(\rho)\, d\rho = s_0 e^{(\gamma_p+\kappa)t}$, increases exponentially fast, a common feature of random sequential processes (Cocke 1969, Hinch 1999, Duplat & Villermaux 2000). **Figure 6** shows examples of this paradigm of sequential mixing, commonplace in real-world and numerical experiments. From $Q(\rho)$, apparent stretching rates $\gamma = (\ln\rho)/t$ [or finite-time Lyapunov exponents (Bohr et al. 1998)] can be defined, whose distribution is

$$G(\gamma) = \sqrt{\frac{t}{4\pi\kappa}}\, e^{-\frac{(\gamma-\gamma_p)^2}{4\kappa}t}, \tag{41.}$$

which shows that, as time proceeds, all elements of the strip progressively experience the same effective stretching given by the most probable stretching rate, γ_p. Cumulated stretching histories are all alike as the mixture approaches uniformity. In a private communication, Kalda suggested (see Meunier & Villermaux 2010) that γ_p and κ should be related to each other by $\gamma_p = d\kappa$ in dimension d; from the sole knowledge of the net growth rate of material surfaces, the entire distribution of elongations can be inferred.

Annu. Rev. Fluid Mech. 2019.51:245-273. Downloaded from www.annualreviews.org
Access provided by University of Oslo - Medical Library on 06/03/20. For personal use only.

Annu. Rev. Fluid Mech. 2019.51:245-273. Downloaded from www.annualreviews.org
Access provided by University of Oslo - Medical Library on 06/03/20. For personal use only.

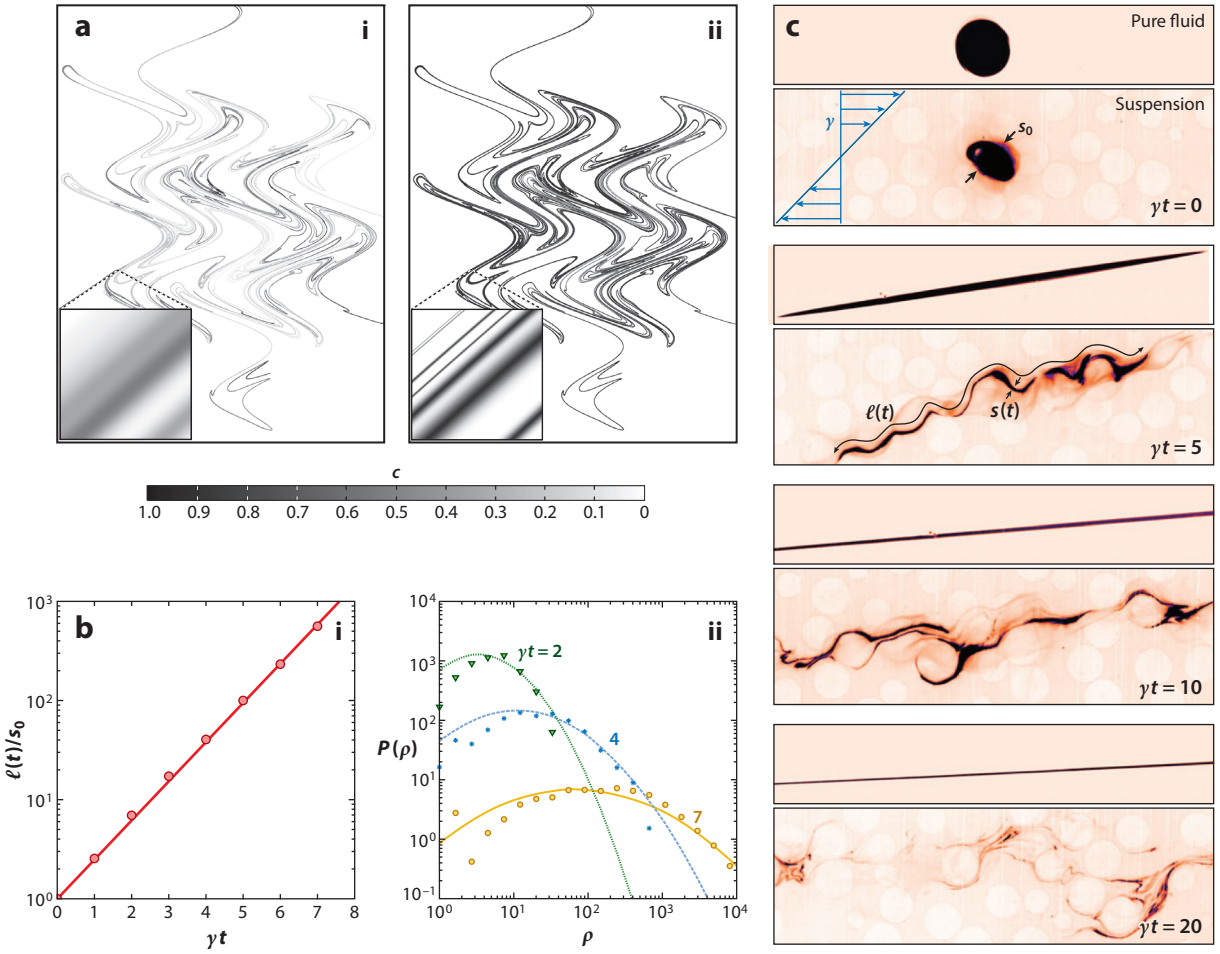

Figure 6

Sequential random stretchings and the log-normal paradigm: mixing a blob by a simulated sine flow. (*a*) The concentration field is reconstructed a posteriori once the kinematics of the deformation and the associated distribution of τ along the strip have been computed. The Péclet number, $Pe = 10^7$ (*i*) and $Pe = 10^8$ (*ii*), is then varied at will, showing how lamellae overlap earlier at lower *Pe*. (*b*) Exponential growth of the lamella length $\ell(t)$ (*i*) and elongation distribution $P(\rho)$ represented by Equation 40 for three successive instants of time (*ii*). (*c*) Blob elongations in a sheared flow without (*top images*) and in the presence of (*bottom images*) a suspension of beads for successive instants of time. The heterogeneity of the local elongations of the strip can be seen. Panels adapted with permission from (*a*,*b*) Meunier & Villermaux (2010) and (*c*) Souzy et al. (2017).

The distributions $q(\theta)$ and $p(c)$ follow from $P(\rho)$ by quadratures (see Equation 39), and since θ, τ, and ρ are power laws of one another in the long-time limit, $p(c)$ is also log-normal (Le Borgne et al. 2015).

3.2.2. Solitary strips in turbulence. The multiplicative nature of the elongation process is such that strongly elongated portions of a blob are likely to be even more stretched in the next sequences. Since large elongation means short mixing time, the distribution of mixing times $T(t_s)$ obtained from Equation 40 with Equations 21 and 39 is an essentially decaying function of t_s, well

Annu. Rev. Fluid Mech. 2019.51:245-273. Downloaded from www.annualreviews.org
Access provided by University of Oslo - Medical Library on 06/03/20. For personal use only.

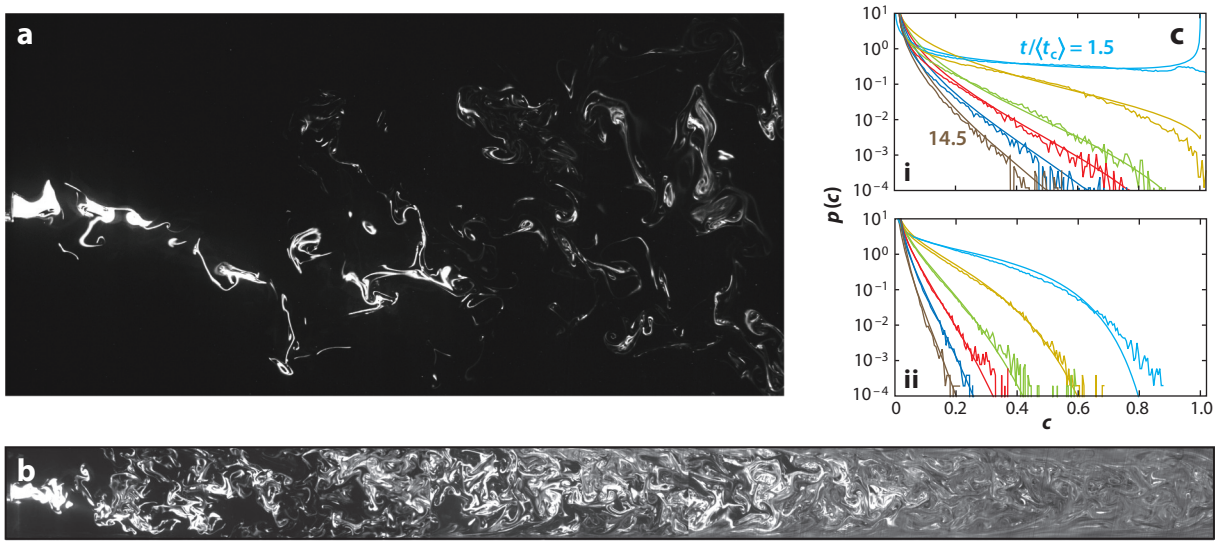

Figure 7

(*a*) A planar cut through a dispersing plume made by the injection of a dye (disodium fluorescein in water) through a small tube, 4 mm in diameter, on the axis of a larger turbulent jet, 8 cm in length. Scalar sheets dilute by evolving on their own. Panel *b* shows the same setup as panel *a*, but with the plume confined in a square duct with a lateral width of 3 cm. The mixture relaxes through the aggregation of sheets, toward a nonzero average concentration; the Reynolds number *Re* is 10^4. (*c*,*i*) Concentration distributions $p(c)$ measured at increasing distances from the source in panel *a*, along with fits from Equation 43 for Schmidt number $Sc = 10^3$. Subpanel *ii* shows the same as subpanel *i*, but with $Sc = 7$ (heat in water). Panels adapted with permission from (*a*,*b*) Le Borgne et al. (2017) and (*c*) Duplat et al. (2010a).

represented by (Shraiman & Siggia 1994; see also Duplat et al. 2010a)

$$T(t_s) = \frac{1}{\langle t_s\rangle} e^{-t_s/\langle t_s\rangle}. \qquad 42.$$

Crossover functions like $\theta \approx (1 + t/t_s)^{-\beta}$ (Duplat et al. 2010a) or $\theta \approx 1 - e^{-(t_s/t)^{\beta}}$ (Le Borgne et al. 2017) are good fits for θ in Equation 20, leading with Equation 33 to (**Figure 7**)

$$p(c) = \frac{\tilde{t}}{\beta} \frac{[-\log(1-c)]^{\frac{1}{\beta}-1}}{1-c} e^{-\tilde{t}[-\log(1-c)]^{\frac{1}{\beta}}}, \quad \text{with} \quad \tilde{t} = \frac{t}{\langle t_s\rangle}. \qquad 43.$$

In the far field of a decaying turbulent jet with mean velocity u, the average mixing time of a solitary strip injected from a tube of diameter h smaller than the radius of the jet is given by $\langle t_s\rangle \sim (h/u)Sc^{1/5}$, for which the Schmidt number dependence was checked over three orders of magnitude. In a turbulent flow, the strip is chopped off in lamellae with thickness of the order of the Taylor scale, $s_0 \sim \sqrt{\nu h/u}$, which are further stretched by the velocity gradient, $\gamma \sim u/h$, at the scale of the injection tube according to $s(t) \sim s_0(\gamma t)^{-2}$; hence we have $Pe = \gamma s_0^2/D = Sc$ and $\beta = 5/2$ (Duplat et al. 2010a; see also Villermaux & Rehab 2000). In a slightly different context, Kalda & Morozenko (2008) proposed a similar construction involving exponentially distributed stretchings at each sequence of fixed duration $\langle t_s\rangle$:

$$p(c) = \frac{(-\ln c)^{\tilde{t}-1}}{\Gamma(\tilde{t})}. \qquad 44.$$

The exponentially decaying form of $p(c > \langle c\rangle) \sim e^{-\tilde{t}c}$ exemplifies rare events that become rarer with increasing time or distance to the source. These intermittent, still-not-mixed portions of the

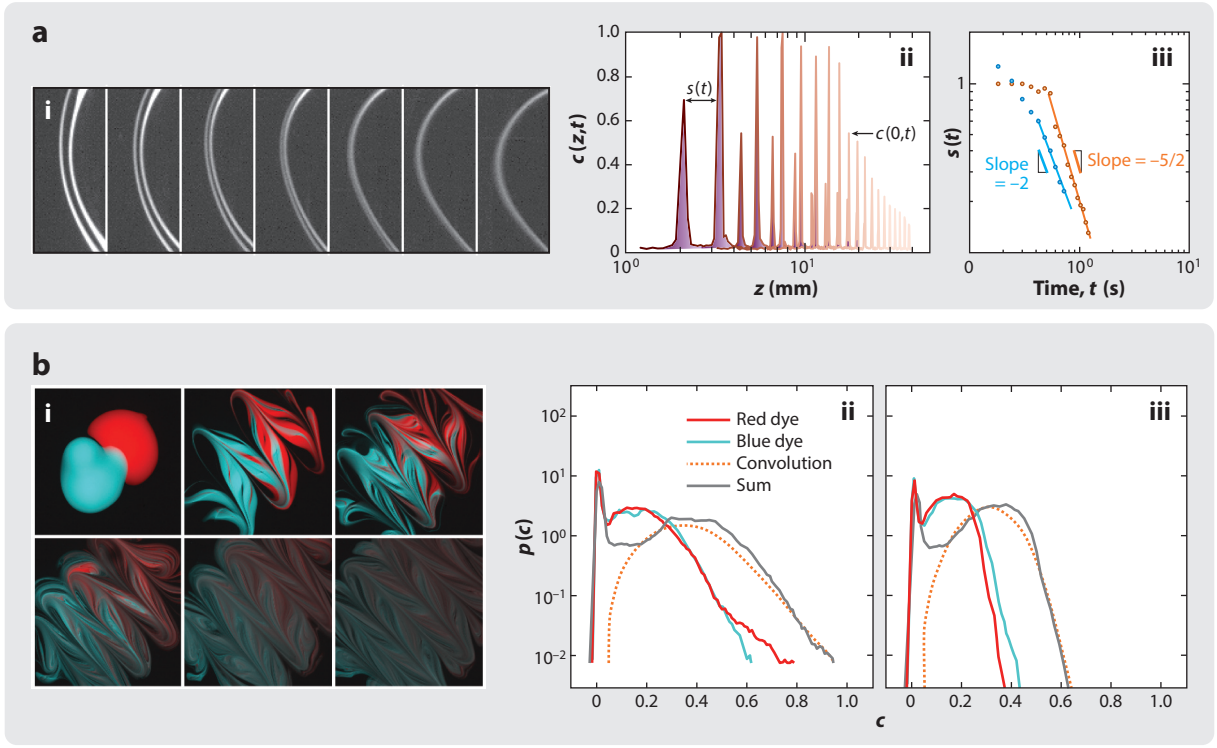

Figure 8

Lamellae overlap and convolutions. (*a*) Lamellae aggregation and temporal evolution of separation distance, $s(t) \sim t^{-2}$, and associated maximal concentration, $\theta \sim t^{-5/2}$. (*b*,*i*) Splitting a blob into two different subparts, dyed red and blue. (*ii*) Concentration distributions $p(c)$ for the red and blue dyes in subpanel *i* (*red and blue lines*) for 5 and 8 stirs, along with their convolution according to Equation 47 (*dotted orange lines*) and the sum of the two fields (*gray lines*). Panels adapted with permission from (*a*) Duplat & Villermaux (2008) and (*b*) Duplat et al. (2010b).

strip separated from each other by immense voids carry a concentration way above the (otherwise close to zero) mean concentration, $\langle c \rangle$ (Celani et al. 2014).

4. OVERLAPS

Solitary strips give a fair representation of the mixture composition as long as each of their subparts evolves on its own, but in most flows in practice, this lonely route has an end: A blob stretched exponentially in a bounded 2D space soon occupies, after t_s, an area $s_0\sqrt{D/\gamma}e^{\gamma t}$ larger than the stirring domain. In turbulent flows, the strip gets corrugated, or rough, at all scales (i.e., fractal), with a fractal dimension depending on both scale (Catrakis & Dimotakis 1996) and time (Villermaux & Gagne 1994, Villermaux & Innocenti 1999, Nicolleau & Elmaihy 2004). The consequences of this inherent, or enforced, confinement are that a strip will unavoidably overlap with itself and that the concentration levels along the strip will then be no more than that of an individual trajectory but will result from interaction with neighboring portions of the strip (**Figure 8**).

Annu. Rev. Fluid Mech. 2019.51:245-273. Downloaded from www.annualreviews.org
Access provided by University of Oslo - Medical Library on 06/03/20. For personal use only.

4.1. Linearity of the Fourier Equation: Additions and Convolutions

The Fourier Equation 18 is linear in c, and any concentration field $c(\xi,\tau)$ is the sum of Gaussian pulses with amplitude modulated by an appropriate initial condition $c(\xi,0)$:

$$c(\xi,\tau)=\int \frac{\mathrm{d}\xi' c(\xi',0)}{2\sqrt{\pi\tau}} e^{-\frac{(\xi-\xi')^2}{4\tau}}. \qquad 45.$$

Equivalently, a mixture is the sum of its subparts: The concentration profile of a set of two lamellae, 1 and 2, such as those shown in **Figure 8** with profiles $c_1(\xi,\tau)$ and $c_2(\xi,\tau)$, respectively, is obtained by summation:

$$c(\xi,\tau)=c_1(\xi,\tau)+c_2(\xi,\tau), \qquad 46.$$

an elementary composition rule that is the building block of the evolution of complex mixtures. Indeed, if one a priori divides a blob in two by tagging each subpart with a different color, and if $p_1(c_1)$ and $p_2(c_2)$ are the concentration distributions of each subfield, then the distribution $p(c)$ of the total concentration field $c=c_1+c_2$ must be a combination of them.

For a broad variety of stirring protocols where the lamellae are enforced to overlap, it has been found that additions in Equation 46 are made at random among the concentration levels available in the current distributions. Random additions in concentration space translate into a convolution in probability space (Feller 1971),

$$p(c)=\int_{c=c_1+c_2} p_1(c_1)p_2(c_2)\,\mathrm{d}c_2 = p_1\otimes p_2, \qquad 47.$$

which, when it actually succeeds at describing the mixture, gives a precise definition of what "random stirring protocol" means. This is the case for interfering line sources (Warhaft 1984) and plumes (Duplat & Villermaux 2008) in turbulence, blobs stirred in viscous fluids (Duplat et al. 2010b), and porous media (Kree & Villermaux 2017). For these stirring protocols, all particles constitutive of the mixture have a chance to interact with all the others. This excludes flows with permanent segregated islands (Giona et al. 2004) or, to some extent, slow regions like those near walls, which prevent good blending (Gouillart et al. 2007).

4.2. Self-Convolution and Gamma Distributions

Solitary strips evolve on their own in dispersing mixtures but, when confined, overlap according to Equation 47. The distribution $p(c,t+\delta t)$ is thus the result of a convolution with itself $p(c,t)$ an instant earlier, which is necessary to complete the summation Equation 46. We confuse c and θ and consider the following two limits, making use of the Laplace transform of $\tilde{p}(s,t)=\int_0^\infty p(c)e^{-sc}\,\mathrm{d}c$:

- A fraction $r\delta t$ of the lamellae or sheets undergoes a complete addition between t and $t+\delta t$, and in that case, we have

$$\partial_t\tilde{p}=r\left(-\tilde{p}+\tilde{p}^2\right), \qquad 48.$$

  an equation familiar in the context of kinetic aggregation since von Smoluchowski (1917) (see also Curl 1963, Pope 1985, Pumir et al. 1991) whose asymptotic solution is a decaying exponential irrespective of $p(c,0)$, broadening in time:

$$p(c,t)\sim \exp\left(-\frac{c}{e^{\int_0^t r\,\mathrm{d}t'}}\right). \qquad 49.$$

- The convolution operation occurs on a continuous timescale everywhere in the flow, with sheets all merging with their neighbors in a continuous way, therefore altering the

Annu. Rev. Fluid Mech. 2019.51:245-273. Downloaded from www.annualreviews.org
Access provided by University of Oslo - Medical Library on 06/03/20. For personal use only.

distribution $p(c,t)$ even on an infinitesimal timescale. In that case, we have

$$\partial_t \tilde{p} = r\tilde{p}\ln\tilde{p}, \qquad 50.$$

whose solution is the self-convolution of the initial distribution $p(c,0)$ as

$$p(c,t) = p(c,0)^{\otimes \exp\left(\int_0^t r dt'\right)}. \qquad 51.$$

The two self-convolution routes above are distinct limits of the general evolution equation (Villermaux & Duplat 2003),

$$\partial_t \tilde{p} = rn\left(-\tilde{p} + \tilde{p}^{1+1/n}\right), \qquad 52.$$

defining for $p(c,t)$ a unique family of distributions, with a single parameter n. The discrete time additions in Equation 48 correspond to $n = 1$, and the uniform continuous time process in Equation 50 is recovered when n tends to infinity. To this crucial random addition step, the decay of c is superimposed by stretching, resulting in a global shift, $p(c+\delta c, t+\delta t) = p(c,t)$ with $\langle \delta c/\delta t\rangle = -\gamma(t)c$, so that the complete evolution of $p(c,t)$ is

$$\partial_t p = \gamma\partial_c (c\ p) + rn\left(-p + p^{\otimes 1+1/n}\right). \qquad 53.$$

In mixtures with conserved average concentration, additions compensate for stretching so that r equals γ, and since the lamellae aggregate because they are stretched, we have $\dot{n} = \gamma n$. The parameter n thus appears as a number of convolutions at time t, and since the piling up of the concentration levels by coalescence through Equation 52 contributes to a concentration increase $\exp\{\int dn/n\} = n$, the average concentration is conserved, provided that

$$n = \frac{1}{\theta(t)}. \qquad 54.$$

In that case, $p(c,t)$ is asymptotically given by a Gamma distribution,

$$p(x = c/\langle c\rangle) = \frac{n^n}{\Gamma(n)}\, x^{n-1}\, e^{-nx}, \quad \text{with} \quad \dot{n}/n = \gamma(t), \qquad 55.$$

with order $n(t)$ increasing in time, which is only a function of the mixture rate of stretch. The shape of the distribution solely reflects the microscopic additions giving birth to it. Obviously, $p(x)$ tends to $\delta(x-1)$ as n tends to infinity when the mixture is completely mixed in the sense of Equation 8 and not simply blended as in Equation 7; it took the above developments to understand why and how.

This distribution well represents mixtures in turbulent channel flows (see Duplat & Villermaux 2008 and **Figure 9**), weakly heterogeneous porous media (Le Borgne et al. 2015), and blobs in viscous fluids (Villermaux & Duplat 2003), along with their respective temporal dependencies of n, specific to each stirring protocol. Numerical simulations have confirmed that the solitary strip concentration distribution has to be convoluted with itself $n(t)$ times to reconstruct the full overlapped mixture $p(c,t)$ (Meunier & Villermaux 2010, Le Borgne et al. 2015).

Additions in Equation 46 should be understood about the mean $\langle c\rangle$ and actually lead to the Gamma family (Equation 55) when $\langle c\rangle$ is significantly less than 1. When $\langle c\rangle = 1/2$, for instance, the fluctuations of $c - \langle c\rangle$ are symmetrical about 0 and Equation 53 leads to Bessel functions (Villermaux et al. 2008).

4.3. Coarsening Scale and Increments

The permanent overlap of lamellae in a stirred mixture has consequences not only for its concentration content but also for its spatial structure.

Annu. Rev. Fluid Mech. 2019.51:245-273. Downloaded from www.annualreviews.org
Access provided by University of Oslo - Medical Library on 06/03/20. For personal use only.

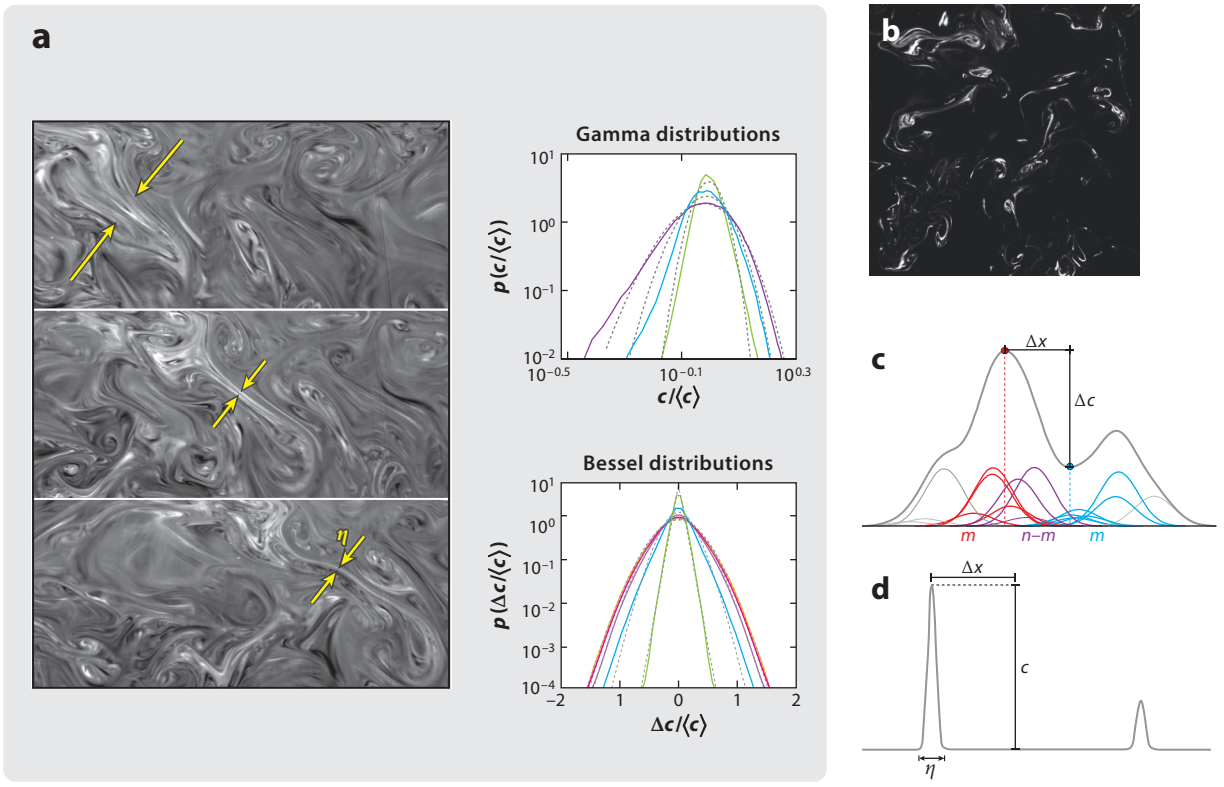

Figure 9

(*a*) Three consecutive instants of time showing how a bundle of stretched sheets in a confined channel are brought together and merge, losing their individuality, on a support of transverse thickness η, leading to Gamma distributions for $p(c/\langle c\rangle)$ in Equation 55 and Bessel distributions for $p(\Delta c/\langle c\rangle)$ in Equation 62. (*b*) Close-up in the dispersing mixture showing how the scalar field resolves into a set of essentially noninteracting, disjointed sheets with distributed concentrations. (*c*) Sketch of the elementary sheet overlapping mechanism constructing the concentration field: Every concentration level c results from the merging of n sheets (the rapidly oscillating curves with concentrations θ) on a support of size η. Nearby concentration levels (separated by Δx) have in common the contribution of $n-m$ sheets. (*d*) In dispersing mixtures where sheets are isolated and merging is anecdotal, concentration differences Δc are given by the concentration field c itself. Figure adapted with permission from Le Borgne et al. (2017).

4.3.1. Coarsening scale. A Batchelor scale is associated with the balance between diffusion and stretching (Section 2.4); overlaps give rise to another, the coarsening scale (Villermaux & Duplat 2006). Sheets and lamellae are typically dense in space in confined mixtures and are locally parallel and aligned in the direction of stretching, forming bundles.

Consider, for instance, an initial scalar field $c(x,0)$ comprising a bundle of parallel lamellae, each separated from its immediate neighbors by a distance s_0 and piled up over a distance of order L where the stretching applies: From $c(x,0) = 1+\cos(2\pi x/s_0)$ for $x \in \{-L/2, L/2\}$, we have $c(\xi,\tau) = 1+\cos(\xi)e^{-\tau}$. The time needed for the lamellae in the bundle to completely coalesce (**Figure 9**) is the time required to make the concentration modulations small compared to unity (i.e., $\tau > 1$). At that time t_s, the bundle where the merged lamella have percolated (Villermaux 2012a, Le Borgne et al. 2017) has shrunk down to the transverse size given by

$$\eta = LPe^{-\alpha/(2\alpha+1)} \qquad 56.$$

Annu. Rev. Fluid Mech. 2019.51:245-273. Downloaded from www.annualreviews.org
Access provided by University of Oslo - Medical Library on 06/03/20. For personal use only.

for a power law stretching or $\eta = LPe^{-1/2}$ for exponential stretching. Within η, which now scales as the stirring scale L and is thus much larger than the Batchelor scale, the concentration is close to uniform. This is the "scale of scrutiny" imagined by Danckwerts (1953) to describe a mixture. This mechanism explains the ramp-cliff-plateau structures notorious in shear flows. There, L-wide regions of nearly uniform concentration are separated by steep cliffs absorbing a concentration difference of the order of the mean (Sreenivasan 1991, Pumir 1994, Warhaft 2000).

4.3.2. Increments: strips as quanta. In confined mixtures, diffusive overlap between elementary lamellae occurs in bundles of transverse size η (Section 4.3.1). There, the concentration $c(\mathbf{x})$ at a point $\mathbf{x}$ results from the random superposition of concentration levels of n elementary strips, each of them with concentration θ_i, as $c(\mathbf{x}) = \sum_{i=1}^{n} \theta_i(\mathbf{x}, t)$, leading for $p(c)$ to the self-convolution construction described in Section 4.2. This aggregation mechanism has consequences for the mixture's spatial structure, measured for instance by the distribution $p(\Delta c)$ of concentration increments, $\Delta c(\Delta\mathbf{x}) = \langle c(\mathbf{x} + \Delta\mathbf{x}) - c(\mathbf{x})\rangle$.

Consider two locations, $\mathbf{x}$ and $\mathbf{x} + \Delta\mathbf{x}$, separated by a distance, $\Delta x < \eta$. There, the concentrations are $c(\mathbf{x}, t)$ and $c(\mathbf{x} + \Delta\mathbf{x}, t)$, respectively, both of which result from the addition of n independent levels θ_i so that we have

$$\Delta c(\Delta\mathbf{x}) = \sum_{i=1}^{n} \theta_i(\mathbf{x} + \Delta\mathbf{x}) - \sum_{i=1}^{n} \theta_i(\mathbf{x}), \qquad 57.$$

the two sums being contributions from elementary lamellae lying in a neighborhood of size η in $\mathbf{x}$ and $\mathbf{x} + \Delta\mathbf{x}$. Thus, when Δx is less than η, the two neighborhoods intersect, with $n - m$ lamellae in the common overlapping region and m independent lamellae in the rest (**Figure 9**). Upon subtraction (Equation 57), the levels from the $n - m$ lamellae that contribute to both concentration levels cancel out, and thus we have (Le Borgne et al. 2017)

$$\Delta c(\Delta x) = \sum_{i=1}^{n-m+m} \theta_i(\mathbf{x} + \Delta\mathbf{x}) - \sum_{i=1}^{n-m+m} \theta_i(\mathbf{x}) \qquad 58.$$

$$= \sum_{i=1}^{m} \theta_i(\mathbf{x} + \Delta\mathbf{x}) - \sum_{i=1}^{m} \theta_i(\mathbf{x}) \qquad 59.$$

$$= c'(\mathbf{x} + \Delta\mathbf{x}) - c'(\mathbf{x}), \qquad 60.$$

where $c'(\mathbf{x} + \Delta\mathbf{x})$ and $c'(\mathbf{x})$ are now two independent concentrations obtained by the random addition of $m \leq n$ independent lamellae in the respective disjointed neighborhoods. Since the concentration levels $c'(\mathbf{x}, t)$ and $c'(\mathbf{x} + \Delta\mathbf{x}, t)$ are now statistically independent, the convolution rule (Equation 47) applies, and we have

$$p(\Delta c) = \int \mathrm{d}c'\; p(c'|m)p(|\Delta c| - c'|m), \qquad 61.$$

where $p(c'|m)$ is the concentration distribution of m aggregated independent lamellae. Using Equation 55 with $\langle c\rangle = n\theta$, we have

$$p(\Delta c) = \frac{1}{\sqrt{\pi}\theta^{2m}\Gamma(m)} \left(\frac{|\Delta c|\theta}{2}\right)^{m-\frac{1}{2}} K_{m-\frac{1}{2}}\left(\frac{|\Delta c|}{\theta}\right), \qquad 62.$$

where $K_{m-\frac{1}{2}}$ is the Bessel function of order $m - \frac{1}{2}$.The number m obviously increases with the separation distance Δx, and m tends to n as Δx tends to η. Equation 61 illustrates how computing increments of concentration in a field made of elementary aggregations deconstructs

Annu. Rev. Fluid Mech. 2019.51:245-273. Downloaded from www.annualreviews.org
Access provided by University of Oslo - Medical Library on 06/03/20. For personal use only.

the direct aggregation process. One probes all the more deeply, or early, in the process so that small-scale increments are considered, since the number of independent lamellae vanishes as Δx tends to zero. When m tends to 1, $p(c|1)$ is a measure of the quantum (Villermaux 2012a), or elementary brick, constructing the concentration field $p(c)$, that is, the solitary strip. The spatial correlation of the concentration field in a confined mixture thus results from an uncorrelated, random superposition of quanta or strips. Their possible entanglement (Duplat et al. 2010b) singles out long-lasting temporal correlations from the mixture's initial condition or stirring protocol.

SUMMARY POINTS

1. Mixing is neither blending nor stirring. Mixing is stretching-enhanced diffusion and results from a subtle interplay between substrate deformation and diffusion broadening when the Péclet number (*Pe*) is large.
2. In most instances involving mixing, the interest is in controlling the probability of large or low concentrations. There is therefore a need to understand the concentration distributions $p(c)$ and especially their large excursion tails.
3. Concentrations c are described by a pure diffusion equation, $\partial_\tau c = \partial_\xi^2 c$, in suitably chosen variables (ξ, τ), a function of the nature of the local stretch history and of molecular diffusion. Concentrations decay after a mixing time, $t_s \sim \gamma^{-1}\mathcal{F}(Pe)$, essentially fixed by the deformation rate of the substrate γ, corrected by a (usually weak but singular) function of *Pe*, depending on the stirring protocol.
4. Stirring motions form lamellae, which are typically unevenly stretched. When these solitary strips evolve on their own, they carry a distribution of concentration $p(c)$, reflecting the elongation histories along the strip only.
5. In confined mixtures where the strips are forced to overlap, concentration levels add at random, and $p(c)$ is constructed by a self-convolution rule determining its shape (a Gamma distribution) and directing its evolution toward uniformity.
6. Bundles of lamellae aggregate at the coarsening length scale η, which is larger than the Batchelor scale, proportional to the stirring scale, and a decaying function of *Pe*. Within a range of scales, $\Delta x \leq \eta$, the distribution of concentration differences $p(\Delta c)$ is a deconstruction of the direct aggregation process, giving birth to $p(c)$.

FUTURE ISSUES

1. Heuristics: The present ideas and methods are not limited to passive scalars. They were successfully applied to evaporating dense sprays (Villermaux et al. 2017) and Marangoni flows (Geri et al. 2017, Néel & Villermaux 2018), should contribute to the reexamination of old problems like mixing in stratified flows (Osborn 1980) or in chemically reactive mixtures (Gibson & Libby 1972, Tél et al. 2005) or the "demixing" of colloids by diffusiophoresis (Preive et al. 1984, Deseigne et al. 2014, Shin et al. 2017, Raynal et al. 2018), and could be applied to mixing by living animals (biomixing; see, e.g., Kurtuldu et al. 2011) or by optimized stirring protocols (Thiffeault 2012, Weij & Bartolo 2017), among other fascinating topics.

Annu. Rev. Fluid Mech. 2019.51:245-273. Downloaded from www.annualreviews.org
Access provided by University of Oslo - Medical Library on 06/03/20. For personal use only.

2. Fundamentals: In confined mixtures, the self-convolution route toward uniformity is an empirical fact. However, the status of this ubiquitous maximal randomness property of random flows is unclear. A simple case using maps could be worked out to understand the decay of correlation of τ in space (hence ensuring the independence of concentrations at merging); this may not be a simple exercise (Gilbert 2006), although it would certainly be a useful one.
3. Numerics: A solitary strip carries concentrations only reflecting its elongation history (i.e., τ). This fact has prompted the diffusive strip method, a simulation method to compute a mixture from the kinematics of the flow a posteriori for $Pe > 1$. Working both in two (Meunier & Villermaux 2010) and in three (Martinez-Ruiz et al. 2018) dimensions, the method could have a broad range of applications.

DISCLOSURE STATEMENT

The author is not aware of any biases that might be perceived as affecting the objectivity of this review.

ACKNOWLEDGMENTS

The concept of self-convolution owes much to an early collaboration with J. Duplat. Precise experiments with P. Meunier and later B. Metzger have strengthened the quantitative lamellar description of mixing and its numerical implementation. The clever simulations by T. Le Borgne and M. Dentz have assessed its relevance for a deeper understanding of complex mixtures. I express my gratitude to all these brilliant colleagues with whom it is always a pleasure to work.

LITERATURE CITED

Allègre CJ, Turcotte DL. 1986. Implications of a two-component marble-cake mantle. *Nature* 323:123–27
Aref H, Blake JR, Budišić M, Cardoso SSS, Cartwright JHE, et al. 2017. Frontiers of chaotic advection. *Rev. Mod. Phys.* 89:025007
Arnold VI, Avez A. 1967. *Problèmes ergodiques de la mécanique classique*. Paris: Gauthier-Villars
Ashurst WT, Kerstein AR, Kerr RM, Gibson CH. 1987. Alignment of vorticity and scalar gradient with strain rate in simulated Navier–Stokes turbulence. *Phys. Fluids* 30:2343–53
Audoly B, Berestycki H, Pomeau Y. 2000. Réaction diffusion en écoulement stationnaire rapide. *C. R. Acad. Sci. IIb* 328:255–62
Balmforth NJ, Young WR. 2003. Diffusion-limited scalar cascades. *J. Fluid Mech.* 482:91–100
Batchelor GK. 1959. Small-scale variation of convected quantities like temperature in a turbulent fluid. Part 1. General discussion and the case of small conductivity. *J. Fluid Mech.* 5:113–33
Beigie D, Leonard A, Wiggins S. 1991. A global study of enhanced stretching and diffusion in chaotic tangles. *Phys. Fluids A* 3:1039–50
Berg HC. 2004. E. coli *in Motion*. New York: Springer-Verlag
Biferale L, Crisanti A, Vergassola M, Vulpiani A. 1995. Eddy diffusivities in scalar transport. *Phys. Fluids* 7:2725–34
Bohr T, Jensen MH, Paladin G, Vulpiani A. 1998. *Dynamical Systems Approach to Turbulence*. Cambridge, UK: Cambridge Univ. Press
Bouchaud JP, Georges A. 1990. Anomalous diffusion in disordered media: statistical mechanisms, models and physical applications. *Phys. Rep.* 195:127–293
Brodkey RS. 1967. *The Phenomena of Fluid Motions*. Reading, MA: Addison-Wesley

Annu. Rev. Fluid Mech. 2019.51:245-273. Downloaded from www.annualreviews.org
Access provided by University of Oslo - Medical Library on 06/03/20. For personal use only.

Annu. Rev. Fluid Mech. 2019.51:245-273. Downloaded from www.annualreviews.org
Access provided by University of Oslo - Medical Library on 06/03/20. For personal use only.

Carrier GF, Fendell FE, Marble FE. 1975. The effect of strain rate on diffusion flames. *SIAM J. Appl. Math.* 28:463–500

Carslaw HS, Jaeger JC. 1959. *Conduction of Heat in Solids*. Oxford: Clarendon. 2nd ed.

Catrakis HJ, Dimotakis PE. 1996. Mixing in turbulent jets: scalar measures and isosurface geometry. *J. Fluid Mech.* 317:369–406

Celani A, Cencini M, Vergassola M, Villermaux E, Vincenzi D. 2005. Shear effects on passive scalar spectra. *J. Fluid Mech.* 523:99–108

Celani A, Villermaux E, Vergassola M. 2014. Odor landscapes in turbulent environments. *Phys. Rev. X* 4:041015

Chandrasekhar S. 1943. Stochastic problems in physics and astronomy. *Rev. Mod. Phys.* 15:1–89

Childress S, Gilbert AD. 1995. *Stretch, Twist, Fold: The Fast Dynamo*. Berlin: Springer-Verlag

Cocke W. 1969. Turbulent hydrodynamic line stretching: consequences of isotropy. *Phys. Fluids* 12:2488–92

Csanady GT. 1973. *Turbulent Diffusion in the Environment*. Dordrecht, Neth.: D. Reidel

Curl RL. 1963. Dispersed phase mixing: I. Theory and effect in simple reactors. *AIChE J.* 9:175–81

Danckwerts PV. 1952. The definition and measurement of some characteristics of mixtures. *Appl. Sci. Res. A* 3:279–96

Danckwerts PV. 1953. Theory of mixtures and mixing. *Research* 6:355–61

de Rivas A, Villermaux E. 2016. Dense spray evaporation as a mixing process. *Phys. Rev. Fluids* 1:014201

Deseigne J, Cottin-Bizonne C, Stroock AD, Bocquet L, Ybert C. 2014. How a "pinch of salt" can tune chaotic mixing of colloidal suspensions. *Soft Matter* 10:4795–99

Donzis DA, Sreenivasan KR, Yeung PK. 2005. Scalar dissipation rate and dissipative anomaly in isotropic turbulence. *J. Fluid Mech.* 532:199–216

Duplat J, Innocenti C, Villermaux E. 2010a. A non-sequential turbulent mixing process. *Phys. Fluids* 22:035104

Duplat J, Jouary A, Villermaux E. 2010b. Entanglement rules for random mixtures. *Phys. Rev. Lett.* 105:034504

Duplat J, Villermaux E. 2000. Persistency of material element deformation in isotropic flows and growth rate of lines and surfaces. *Eur. Phys. J. B* 18:353–61

Duplat J, Villermaux E. 2008. Mixing by random stirring in confined mixtures. *J. Fluid Mech.* 617:51–86

Epstein IR. 1990. Shaken, stirred—but not mixed. *Nature* 346:16–17

Falkovich G, Gawedzki K, Vergassola M. 2001. Particles and fields in fluid turbulence. *Rev. Mod. Phys.* 73:913–75

Fannjiang A, Nonnenmacher S, Wolonski L. 2004. Dissipation time and decay of correlations. *Nonlinearity* 17:1481–508

Favre AE. 1962. *Mécanique de la turbulence*. Paris: Ed. Cent. Natl. Res. Sci.

Feller W. 1971. *An Introduction to Probability Theory and Its Applications*, Vol. 2. New York: Wiley

Figueroa A, Meunier P, Cuevas S, Villermaux E, Ramos E. 2014. Chaotic advection at large Péclet number: electromagnetically driven experiments, numerical simulations, and theoretical predictions. *Phys. Fluids* 26:013601

Fourier J. 1822. *Théorie analytique de la chaleur*. Paris: Firmin Didot

Geri M, Keshavarz B, McKinley GH, Bush JWM. 2017. Thermal delay of drop coalescence. *J. Fluid Mech.* 833:R3

Gibbs JW. 1902. *Elementary Principles in Statistical Mechanics*. New Haven, CT: Yale Univ. Press

Gibson CH, Libby PA. 1972. On turbulent flows with fast chemical reactions. Part II. The distribution of reactants and products near a reacting surface. *Combust. Sci. Technol.* 6:29–35

Gilbert AD. 2006. Advected fields in maps—III. Passive scalar decay in baker's maps. *Dyn. Syst.* 21:25–71

Giona M, Adrover A, Cerbelli S, Vitacolonna V. 2004. Spectral properties and transport mechanisms of partially chaotic bounded flows in the presence of diffusion. *Phys. Rev. Lett.* 92:114101

Gouillart E, Kuncio N, Dauchot O, Dubrulle B, Roux S, Thiffeault JL. 2007. Walls inhibit chaotic mixing. *Phys. Rev. Lett.* 99:114501

Hinch EJ. 1999. Mixing: turbulence and chaos—an introduction. In *Mixing Chaos and Turbulence*, ed. H Chaté, E Villermaux, J-M Chomaz, pp. 37–56. New York: Springer Sci. Bus. Media

Kalda J. 2000. Simple model of intermittent passive scalar turbulence. *Phys. Rev. Lett.* 84:471–74

Kalda J, Morozenko A. 2008. Turbulent mixing: the roots of intermittency. *New J. Phys.* 10:093003

Kitanidis PK. 1994. The concept of the dilution index. *Water Resour. Res.* 30:2011–26

Koehl MAR, Koseff JR, Crimaldi JP, McCay MG, Cooper T, et al. 2001. Lobster sniffing: antennule design and hydrodynamic filtering of information in an odor plume. *Science* 294:1948–51
Kraichnan RH. 1994. Anomalous scaling of a randomly advected passive scalar. *Phys. Rev. Lett.* 72:1016
Kree M, Villermaux E. 2017. Scalar mixtures in porous media. *Phys. Rev. Fluids* 2:104502
Kurtuldu H, Guasto JS, Johnson KA, Gollub JP. 2011. Enhancement of biomixing by swimming algal cells in two-dimensional films. *PNAS* 108:10391–95
Landau L, Lifshitz E. 1987. *Fluid Mechanics*. Oxford: Pergamon
Le Borgne T, Dentz M, Villermaux E. 2015. The lamellar description of mixing in porous media. *J. Fluid Mech.* 770:458–98
Le Borgne T, Huck PD, Dentz M, Villermaux E. 2017. Scalar gradients in stirred mixtures and the deconstruction of random fields. *J. Fluid Mech.* 812:578–610
Levèque MA. 1928. Les lois de la transmission de la chaleur par convection. *Ann. Mines* 13:201–39
Mafra-Neto A, Cardé RT. 1994. Fine-scale structure of pheromone plumes modulates upwind orientation of flying moths. *Nature* 369:142–44
Marble FE. 1964. *Spacecraft propulsion*. Tech. Rep. ST-3, Calif. Inst. Technol., Pasadena, CA
Marble FE. 1988. Mixing, diffusion and chemical reaction of liquids in a vortex field. In *Chemical Reactivity in Liquids: Fundamental Aspects*, ed. M Moreau, P Turq, pp. 581–606. New York: Plenum
Marble FE, Broadwell JE. 1977. *The coherent flame model for turbulent chemical reactions*. Tech. Rep. TRW-9-PU, Project SQUID, Purdue Univ., West Lafayette, IN
Martinez-Ruiz D, Meunier P, Favier B, Duchemin L, Villermaux E. 2018. The diffusive sheet method for scalar mixing. *J. Fluid Mech.* 837:230–57
Matheron G, de Marsilly G. 1980. Is transport in porous media always diffusive? A counterexample. *Water Resour. Res.* 16:901–17
Mathew G, Mezic I, Petzold L. 2005. A multiscale measure for mixing. *Physica D* 211:23–46
Maxwell JC. 1867. On the dynamical theory of gases. *Philos. Trans. R. Soc. Lond.* 157:49–88
McKenzie D. 1979. Finite deformation during fluid flow. *Geophys. J. R. Astron. Soc.* 58:689–715
Meunier P, Huck P, Nobili C, Villermaux E. 2015. Transport and diffusion around a homoclinic point. In *Chaos, Complexity and Transport: Proceedings of the CCT'15*, ed. X Leoncini, C Eloy, G Boedec, pp. 152–62. Singapore: World Sci.
Meunier P, Villermaux E. 2003. How vortices mix. *J. Fluid Mech.* 476:213–22
Meunier P, Villermaux E. 2007. Van Hove singularities in probability density functions of scalars. *C. R. Méc.* 335:162–67
Meunier P, Villermaux E. 2010. The diffusive strip method for scalar mixing in two dimensions. *J. Fluid Mech.* 662:134–72
Miller PL, Dimotakis PE. 1996. Measurements of scalar power spectra in high Schmidt number turbulent jets. *J. Fluid Mech.* 308:129–46
Moffatt HK. 1983. Transport effects associated with turbulence with particular attention to the influence of helicity. *Rep. Prog. Phys.* 46:621–64
Mohr WD, Saxton RL, Jepson CH. 1957. Mixing in laminar-flow systems. *Ind. Eng. Technol.* 49:1855–56
Nagata S. 1975. *Mixing: Principles and Applications*. New York: Wiley
Néel B, Villermaux E. 2018. The spontaneous puncture of thick liquid films. *J. Fluid Mech.* 838:192–221
Nicolleau FCGA, Elmaihy A. 2004. Study of the development of three-dimensional sets of fluid particles and iso-concentration fields using kinematic simulation. *J. Fluid Mech.* 517:229–49
Okubo A, Karweit M. 1969. Diffusion from a continuous source in a uniform shear flow. *Limnol. Oceanogr.* 14:514–20
Osborn TR. 1980. Estimates of the local rate of vertical diffusion from dissipation measurements. *J. Phys. Oceanogr.* 10:83–89
Ott E, Antonsen TM. 1989. Fractal measures of passively convected vector fields and scalar gradients in chaotic fluid flows. *Phys. Rev. A* 39:3660–71
Ottino JM. 1982. Description of mixing with diffusion and reaction in terms of the concept of material surfaces. *J. Fluid Mech.* 114:83–103
Pope SB. 1985. PDF methods for turbulent reacting flows. *Prog. Energy Combust. Sci.* 11:119–92

Annu. Rev. Fluid Mech. 2019.51:245-273. Downloaded from www.annualreviews.org
Access provided by University of Oslo - Medical Library on 06/03/20. For personal use only.

Poulain S, Villermaux E, Bourouiba L. 2018. Ageing and burst of surface bubbles. *J. Fluid Mech.* 851:636–71
Prieve DC, Anderson JL, Ebel JP, Lowell ME. 1984. Motion of a particle generated by chemical gradients. Part 2. Electrolytes. *J. Fluid Mech.* 148:247–69
Pumir A. 1994. A numerical study of the mixing of a passive scalar in three dimensions in the presence of a mean gradient. *Phys. Fluids* 6:2118–32
Pumir A, Shraiman BI, Siggia ED. 1991. Exponential tails and random advection. *Phys. Rev. Lett.* 66:2984–87
Ranz WE. 1979. Application of a stretch model to mixing, diffusion and reaction in laminar and turbulent flows. *AIChE J.* 25:41–47
Raynal F, Bourgoin M, Cottin-Bizonne C, Ybert C, Volk R. 2018. Advection and diffusion in a chemically induced compressible flow. *J. Fluid Mech.* 847:228–43
Reif F. 1965. *Fundamentals of Statistical and Thermal Physics*. Long Grove, IL: Waveland
Rhines PB, Young WR. 1983. How rapidly is a passive scalar mixed within closed streamlines? *J. Fluid Mech.* 133:133–45
Richardson LF. 1926. Atmospheric diffusion shown on a distance-neighbour graph. *Proc. R. Soc. Lond. A* 110:709–37
Rom-Kedar V, Leonard A, Wiggins S. 1990. An analytical study of transport, mixing and chaos in an unsteady vortical flow. *J. Fluid Mech* 214:347–94
Schnitzer MJ, Block SM, Berg HC, Purcell EM. 1990. Strategies for chemotaxis. In *Biology of the Chemotactic Response*, ed. JP Armitage, JM Lackie, pp. 15–33. Cambridge, UK: Cambridge Univ. Press
Schumacher J, Sreenivasan KR, Yeung PK. 2005. Very fine structures in scalar mixing. *J. Fluid Mech.* 531:113–22
Shin S, Shardt O, Warren PB, Stone HA. 2017. Membraneless water filtration using CO_2. *Nat. Commun.* 8:15181
Shraiman BI. 1987. Diffusive transport in a Rayleigh-Bénard convection cell. *Phys. Rev. A* 36:261–67
Shraiman BI, Siggia ED. 1994. Lagrangian path integrals and fluctuations in random flows. *Phys. Rev. E* 49:2912–27
Shraiman BI, Siggia ED. 2000. Scalar turbulence. *Nature* 405:639–46
Solomon TH, Gollub JP. 1988. Passive transport in steady Rayleigh–Bénard convection. *Phys. Fluids* 31:1372–79
Souzy M, Lhuissier H, Villermaux E, Metzger B. 2017. Stretching and mixing in sheared particulate suspensions. *J. Fluid Mech.* 812:611–35
Souzy M, Zaier I, Lhuissier H, Le Borgne T, Metzger B. 2018. Mixing lamellae in a shear flow. *J. Fluid Mech.* 838:R3
Sreenivasan KR. 1991. On local isotropy of passive scalars in turbulent shear flows. *Proc. R. Soc. Lond. A* 434:165–82
Sturman R, Ottino JM, Wiggins S. 2006. *The Mathematical Foundations of Mixing*. Cambridge, UK: Cambridge Univ. Press
Taylor GI. 1953. Dispersion of soluble matter in solvent flowing slowly through a tube. *Proc. R. Soc. Lond. A* 219:186–203
Tél T, de Moura A, Grebogi C, Károlyi G. 2005. Chemical and biological activity in open flows: a dynamical system approach. *Phys. Rep.* 413:91–196
Thiffeault JL. 2004. Stretching and curvature of material lines in chaotic flows. *Physica D* 198:169–81
Thiffeault JL. 2008. Scalar decay in chaotic mixing. In *Transport and Mixing in Geophysical Flows*, ed. JB Weiss, A Provenzale, pp. 3–36. Berlin: Springer-Verlag
Thiffeault JL. 2012. Using multiscale norms to quantify mixing and transport. *Nonlinearity* 25:R1
Vidick B. 1989. Critical mixing parameters for good control of cement slurry quality. *J. Petrol. Technol.* 42(7):924–28
Villermaux E. 2012a. Mixing by porous media. *C. R. Méc.* 340:933–43
Villermaux E. 2012b. On dissipation in stirred mixtures. *Adv. Appl. Mech.* 45:91–107
Villermaux E, Duplat J. 2003. Mixing as an aggregation process. *Phys. Rev. Lett.* 91:184501
Villermaux E, Duplat J. 2006. Coarse grained scale of turbulent mixtures. *Phys. Rev. Lett.* 97:144506
Villermaux E, Gagne Y. 1994. Line dispersion in homogeneous turbulence: stretching, fractal dimensions, and micromixing. *Phys. Rev. Lett.* 73:252–55

Annu. Rev. Fluid Mech. 2019.51:245-273. Downloaded from www.annualreviews.org
Access provided by University of Oslo - Medical Library on 06/03/20. For personal use only.

Villermaux E, Innocenti C. 1999. On the geometry of turbulent mixing. *J. Fluid Mech.* 393:123–45
Villermaux E, Moutte A, Amielh M, Meunier P. 2017. Fine structure of the vapor field in evaporating dense sprays. *Phys. Rev. Fluids* 2:074501
Villermaux E, Rehab H. 2000. Mixing in coaxial jets. *J. Fluid Mech.* 425:161–85
Villermaux E, Stroock AD, Stone HA. 2008. Bridging kinematics and concentration content in a chaotic micromixer. *Phys. Rev. E* 77:015301
von Smoluchowski M. 1917. Versuch einer mathematischen Theorie der Koagulationskinetik kolloider Lösungen. *Z. Phys. Chem.* 92:129–68
Warhaft Z. 1984. The interference of thermal fields from line sources in grid turbulence. *J. Fluid Mech.* 144:363–87
Warhaft Z. 2000. Passive scalars in turbulent flows. *Annu. Rev. Fluid Mech.* 32:203–40
Weij JH, Bartolo D. 2017. Mixing by unstirring: hyperuniform dispersion of interacting particles upon chaotic advection. *Phys. Rev. Lett.* 119:048002
Zel'dovich YB. 1937. The asymptotic law of heat transfer at small velocities in the finite domain problem. *Zh. Eksp. Teor. Fiz.* 7:1466–68

Annu. Rev. Fluid Mech. 2019.51:245-273. Downloaded from www.annualreviews.org
Access provided by University of Oslo - Medical Library on 06/03/20. For personal use only.

Annual Review of
Fluid Mechanics

Volume 51, 2019

Contents

Annu. Rev. Fluid Mech. 2019.51:245-273. Downloaded from www.annualreviews.org
Access provided by University of Oslo - Medical Library on 06/03/20. For personal use only.

Indexes

Errata

An online log of corrections to *Annual Review of Fluid Mechanics* articles may be found at http://www.annualreviews.org/errata/fluid

Annu. Rev. Fluid Mech. 2019.51:245-273. Downloaded from www.annualreviews.org
Access provided by University of Oslo - Medical Library on 06/03/20. For personal use only.